

Transmission Electron Microscopy

-TEM-

The first electron microscope was built 1932 by the German physicist Ernst Ruska, who was awarded the Nobel Prize in 1986 for its invention. He knew that electrons possess a wave aspect, so he believed he could treat them in a fashion similar to light waves. Ruska was also aware that magnetic fields could affect electron trajectories, possibly focusing them as optical lenses do to light. After confirming these principles through research, he set out to design the electron microscope. Ruska had deduced that an electron microscope would be much more powerful than an ordinary optical microscope since electron waves were shorter than ordinary light waves and electrons would allow for greater magnification and thus to visualize much smaller structures. The first crude electron microscope was capable of magnifying objects 400 times. The first practical electron microscope was built by in 1938 and had 10 nm resolution. Although modern electron microscopes can magnify an object 2 million times, they are still based upon Ruska's prototype and his correlation between wavelength and magnification. The electron microscope is now an integral part of many laboratories. Researchers use it to examine biological materials (such as microorganisms and cells), a variety of large molecules, medical biopsy samples, metals and crystalline structures, and the characteristics of various surfaces.

Electron Microscopy

Aim of the lecture



Electron Microscopy is a very large and specialist field

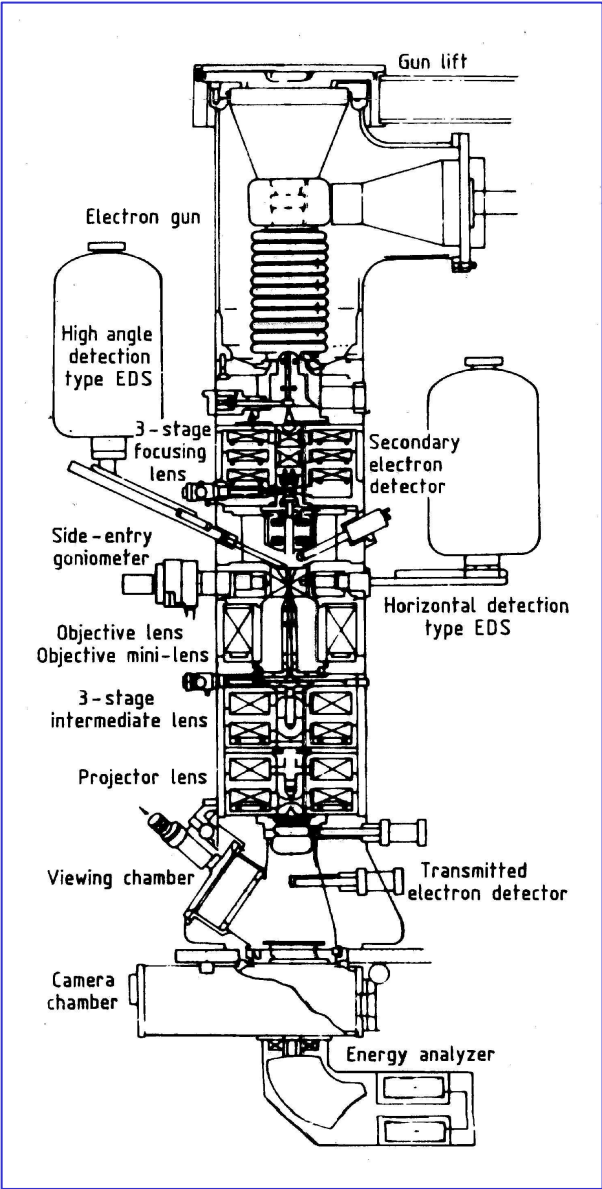
- Just a few information on
- What is it possible to do
 - How do instruments work

History of TEM

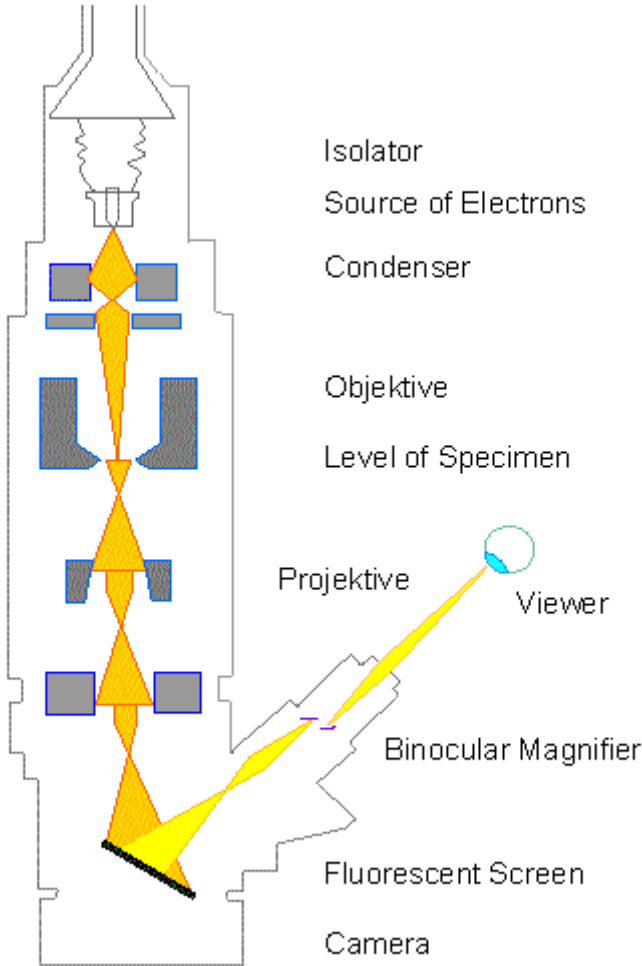
HISTORY OF THE TRANSMISSION **ELECTRON** MICROSCOPE (**TEM**)

- 1897 J. J. Thompson Discovers the **electron**
- 1924 Louis de Broglie identifies the wavelength for electrons as $\lambda=h/mv$
- 1926 H. Busch Magnetic or electric fields act as lenses for electrons
- 1929 E. Ruska Ph.D thesis on magnetic lenses
- 1931 Knoll & Ruska 1st **electron** microscope (EM) built
- 1931 Davisson & Calbrick Properties of electrostatic lenses
- 1934 Driest & Muller Surpass resolution of the Light Microscope
- 1938 von Borries & Ruska First practical EM (Siemens) - 10 nm resolution
- 1940 RCA Commercial EM with 2.4 nm resolution
- 2000 new developments, cryomicroscopes, primary energies up to 1 MeV

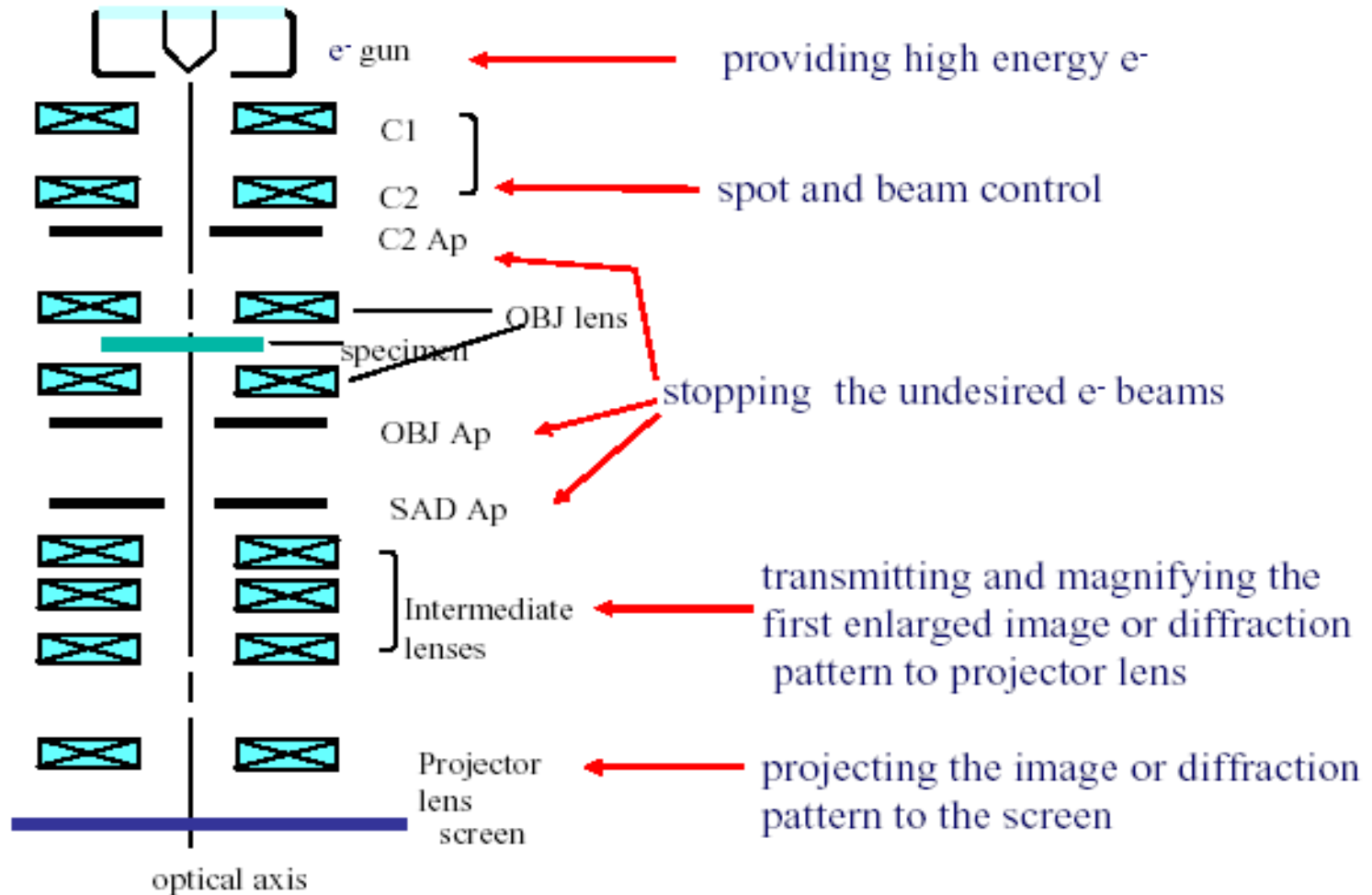
Scheme of TEM



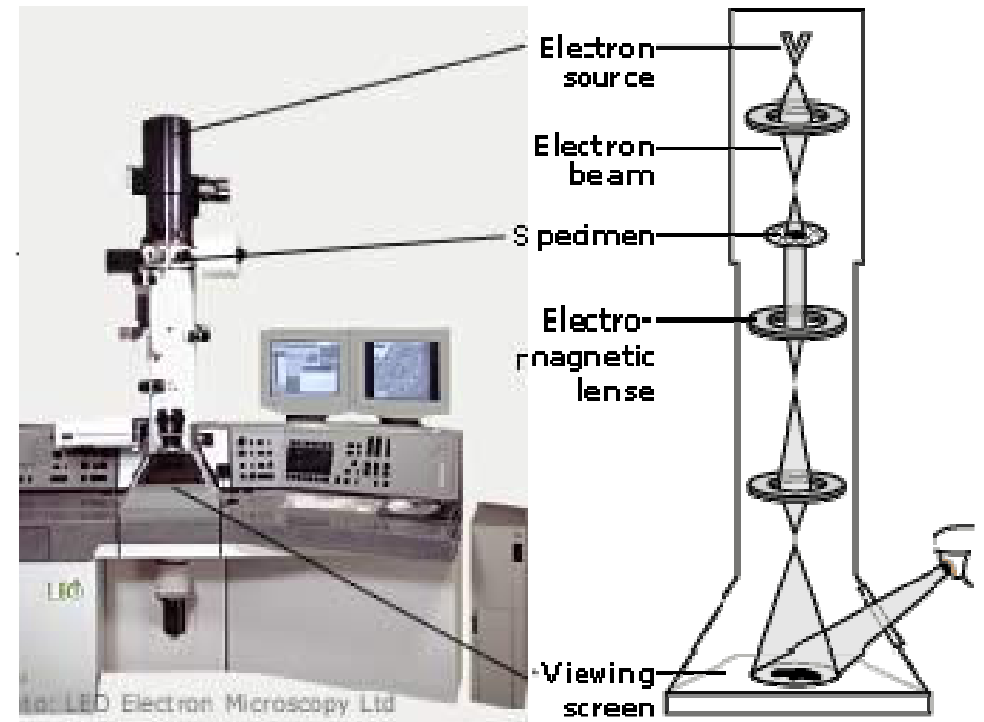
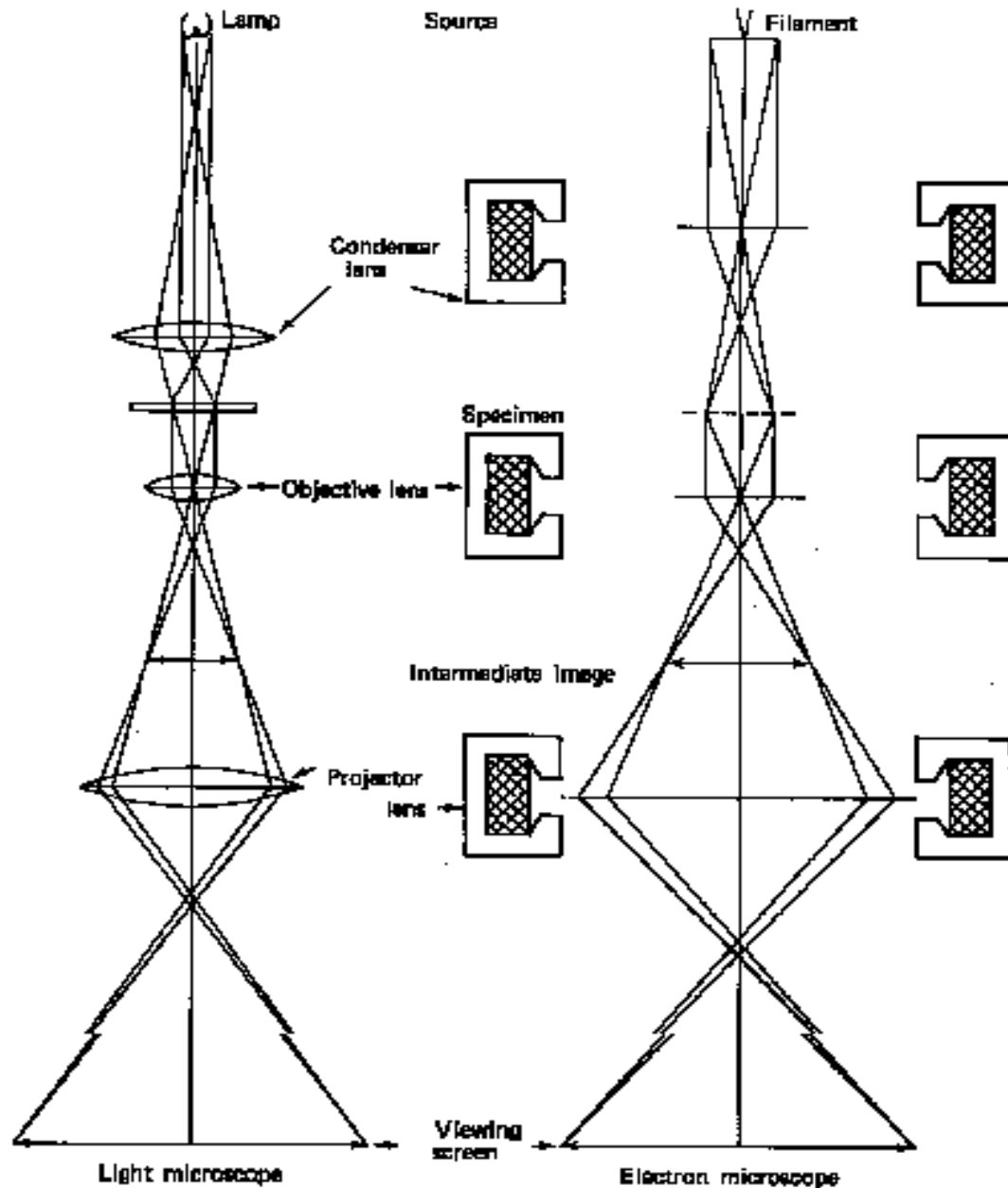
Electrons at 200kV	
Wavelength (nm)	Resolution (nm)
0.00251	~0.2



TEM lens system



Application of magnetic Lenses: Transmission Electron Microscope (Ruska and Knoll 1931) 1945 - 1nm resolution



Basis of the transmission electron microscopy

$$\left. \begin{aligned}
 \lambda &= \frac{h}{m_0 v} \\
 eV &= \frac{1}{2} m_0 v^2 \\
 m_0 &= m \sqrt{\left(1 - \frac{v^2}{c^2}\right)}
 \end{aligned} \right\} \lambda = \frac{h}{\left[2m_0 eV \left(1 + \frac{eV}{2m_0 c^2}\right)\right]^{\frac{1}{2}}}$$



Accelerating voltage (kV)	Nonrelativistic λ (nm)	Relativistic λ (nm)	Velocity ($\times 10^8$ m/s)
100	0.00386	0.00370	1.644
200	0.00273	0.00251	2.086
400	0.00193	0.00164	2.484
1000	0.00122	0.00087	2.823

Resolution

$$r_{th} = 0.61 \frac{\lambda}{\beta} \quad \Rightarrow$$

β = semi-collection angle of magnifying lens

Wavelength (nm)	
Green light	Electrons at 200kV
~550	0.00251

The resolution of the transmission electron microscope is strongly reduced by lens aberration (mainly spherical aberration C_s)

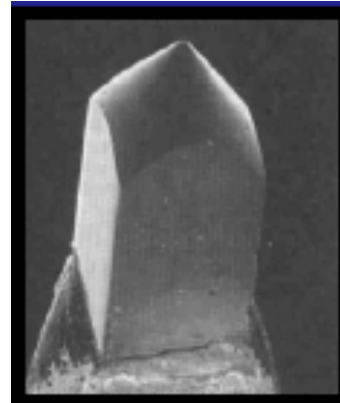
$$r = 0.67 \lambda^{\frac{3}{4}} C_s^{\frac{1}{4}} \quad \Rightarrow$$

Best attained resolution ~0.07 nm
Nature (2006)

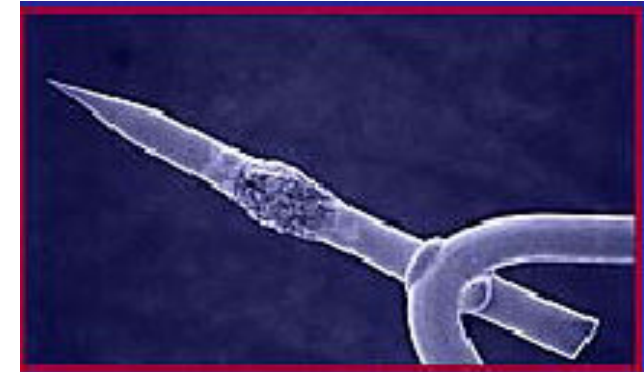
Emitters



tungsten



Lanthanum
hexaboride



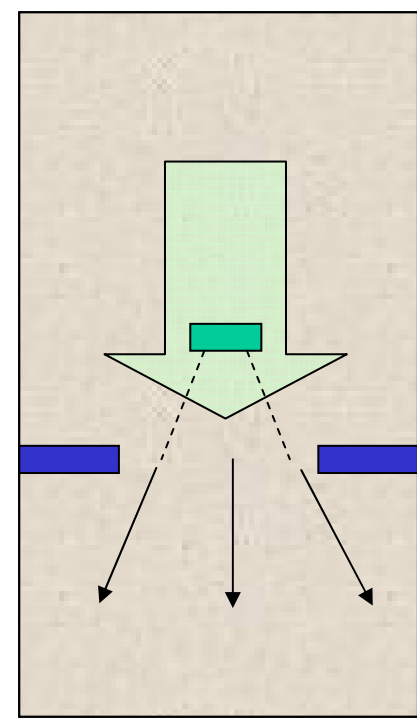
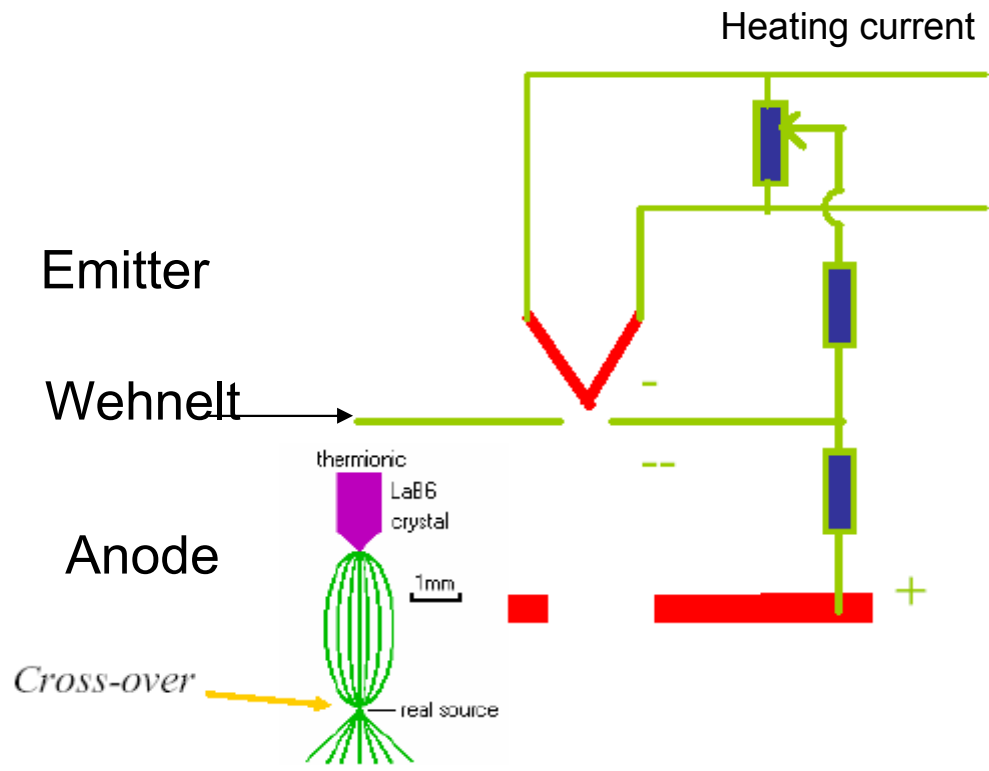
Field emitters: single oriented
crystal of tungsten
etched to a fine tip

SEM Cathode Comparison

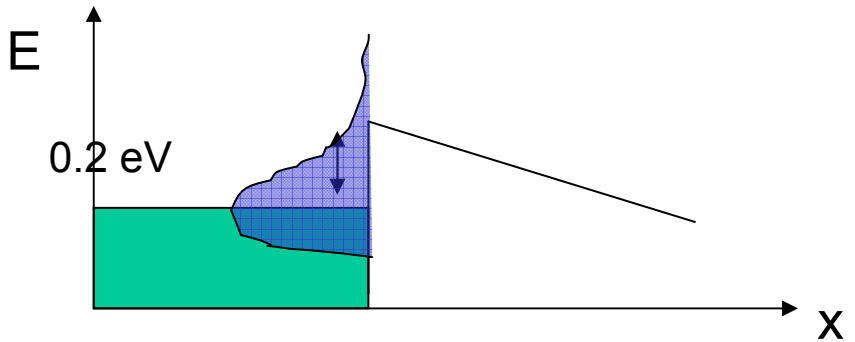
	Tungsten filament	LaB ₆	Schottky (TF)	Field Emission
Apparent Source Size	100 micrometers	5 micrometers	<100 Angstroms	<100 Angstroms
Brightness	1 A/cm ² steradian	20-50 A/cm ² steradian	100-500 A/cm ² steradian	100-1000 A/cm ² steradian
Vacuum Required	10 ⁻⁵ Torr	10 ⁻⁶ Torr	10 ⁻⁸ Torr	10 ⁻⁹ Torr

Table 1 - Gun comparisons

Thermoionic emitters



A virtual probe of size d can be assumed to be present at the first cross-over



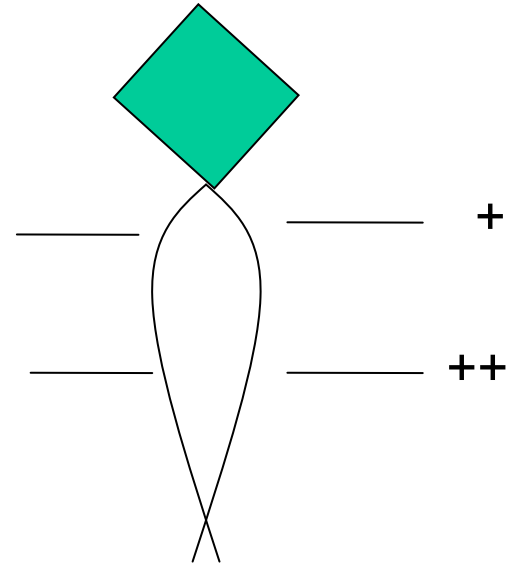
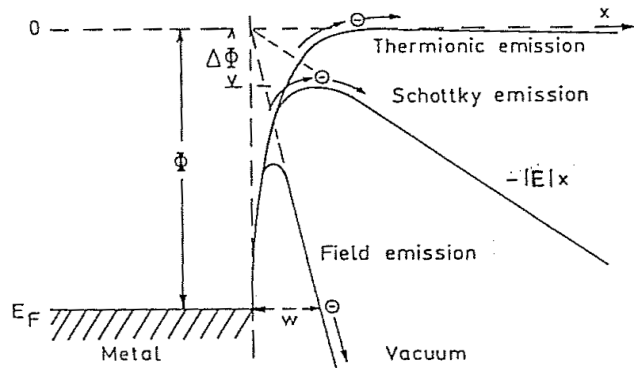
$$J = \frac{4i_c}{d_0^2 \pi}$$

$$J = AT^2 e^{-\frac{\Phi}{KT}}$$

Brightness or Brillance: density per unit solid angle

$$\beta = \frac{4i_c}{d_0^2 \pi \Omega}$$

Schottky and Field emission guns



Emission occurs by tunnel effect

$$J = 6.2 \times 10^6 \sqrt{\frac{\mu}{\Phi}} \frac{E^2}{\mu + \Phi} e^{-\left[6.8 \times 10^4 \frac{\Phi^{1.5}}{E}\right]}$$

E =electric field

Φ =work function

μ =Fermi level

- High brilliance
- Little cross over
- Little integrated current



Coherence

Coherence: A prerequisite for interference is a superposition of wave systems whose **phase difference remains constant in time**. Two beams are **coherent** if, when combined, they produce an interference pattern.

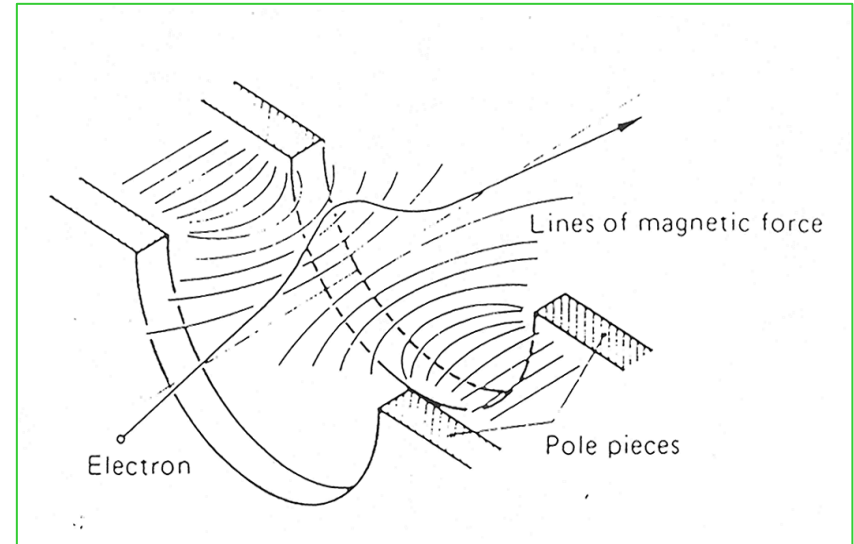
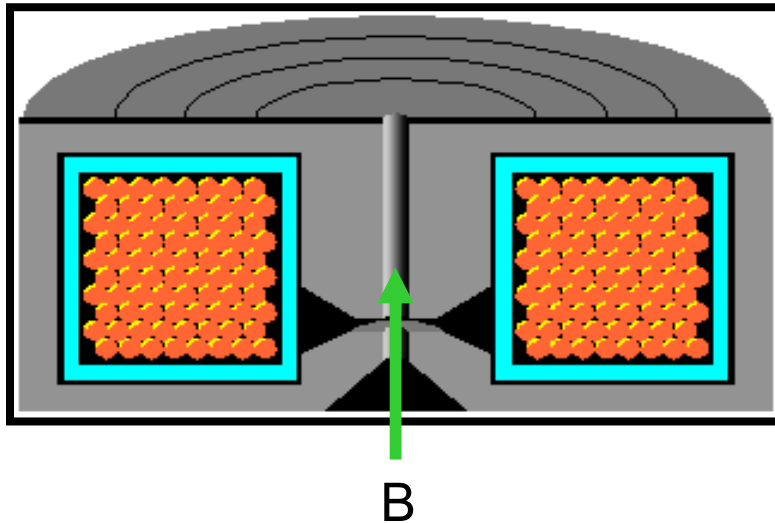
Two beams of light from self luminous sources are incoherent.

In practice an emitting source has finite extent and each point of the source can be considered to generate light. Each source gives rise to a system of Fresnel fringes at the edge. The superposition of these fringe systems is fairly good for the first maxima and minima but farther away from the edge shadow the overlap of the fringe patterns becomes sufficiently random to make the fringes disappear.

The smaller is the source the larger is coherence

Using a beam with more than one single wave vector k reduces the coherence

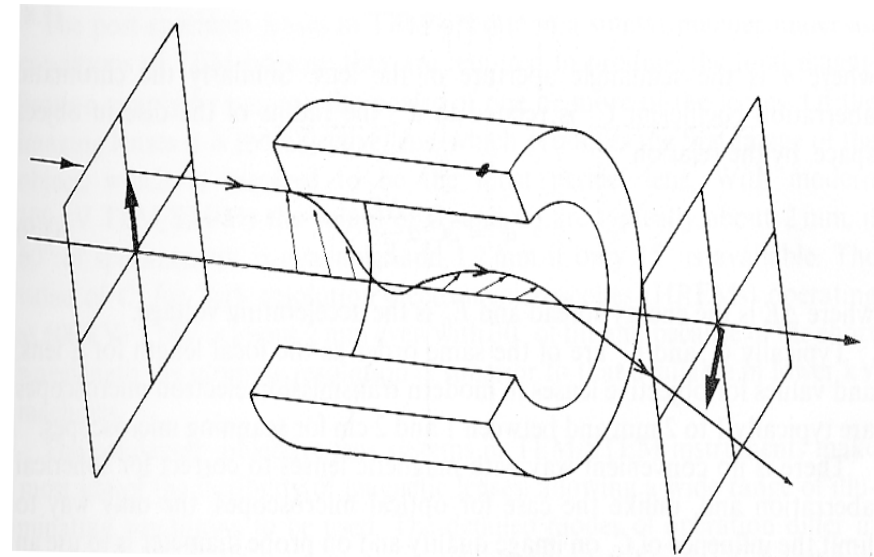
Magnetic lenses



It is a lens with focal length f
but with a rotation θ

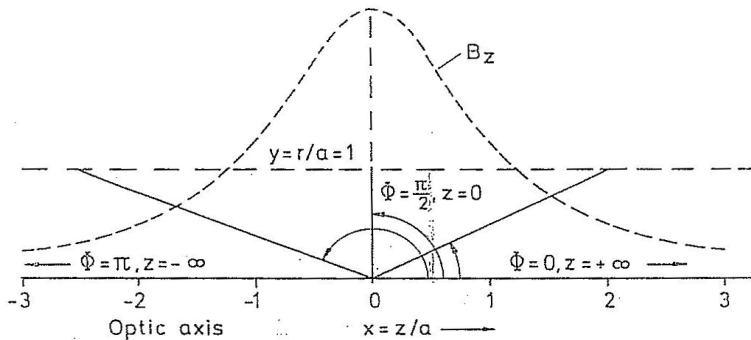
$$\frac{1}{f} = \frac{\eta}{8V} \int_{-\infty}^{+\infty} B^2(x) dx$$

$$\theta = \sqrt{\frac{\eta}{8V} \int_{-\infty}^{+\infty} B(x) dx}$$



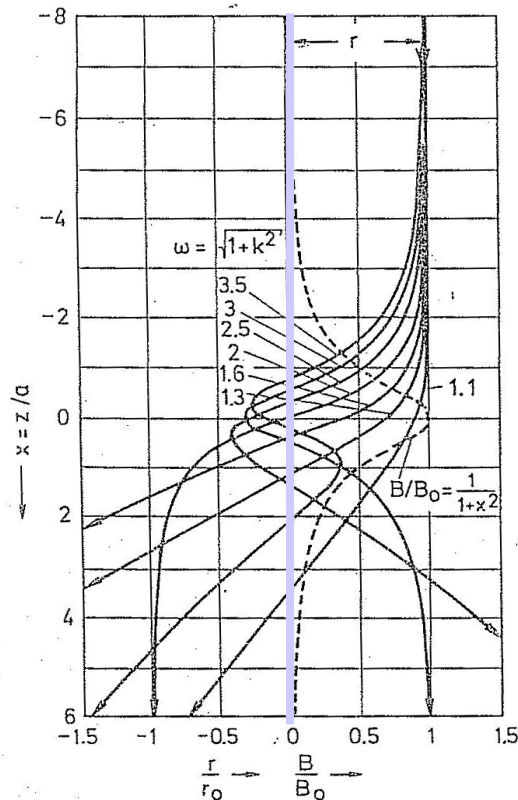
Magnetic lenses: bell shaped field

$$B_z = \frac{B_0}{1 + (z/a)^2} \quad B_r = -\frac{r}{2} \frac{\partial B_z}{\partial z}$$



Newton's law

- 1) $m\ddot{r} = F_r + mr\dot{\phi}^2 = -eB_z r \dot{\phi} + mr \dot{\phi}^2$
- 2) $\frac{d}{dt}(mr^2 \dot{\phi}) = rF_\phi = \frac{d}{dt} \left(\frac{e}{2} r^2 B_z \right)$
- 3) $m\ddot{z} = F_z = eB_r r \dot{\phi}$



from 2): $mr^2 \dot{\phi} = \frac{e}{2} r^2 B_z + C$ with $C=0$ for per trajectories in meridian planes

$$\dot{\phi} = \frac{e}{2m} B_z$$

from 1): $m\ddot{r} = -eB_z r \frac{e}{2m} B_z + mr \left(\frac{e}{2m} B_z \right)^2 = -\frac{e^2}{4m} B_z^2 r$

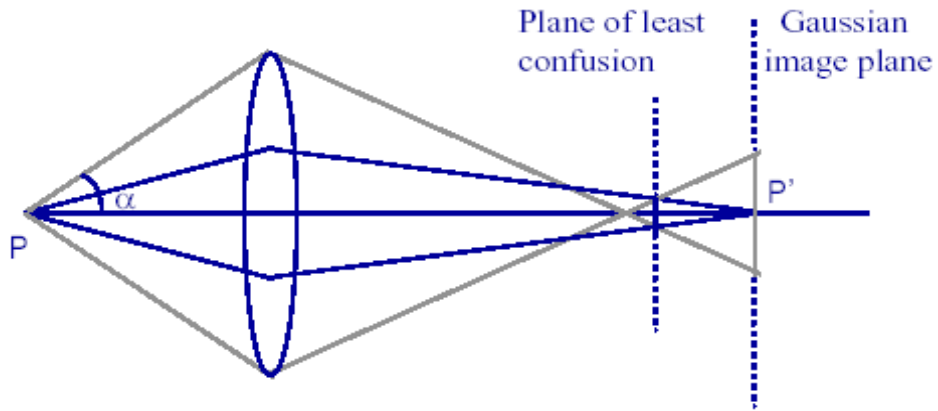
B_r is small for paraxial trajectories, eq. 3) gives $v_z = \text{const}$, while the coordinate r oscillates with frequency $\omega = \sqrt{1+k^2}$

$$\begin{aligned} x &= z/a \\ y &= r/a \end{aligned}$$

$$k^2 = \frac{eB_0^2 a^2}{8m_0 U^*}$$

$$\frac{d^2 y}{dx^2} = -\frac{k^2}{(1+x^2)^2} y$$

Aberrations



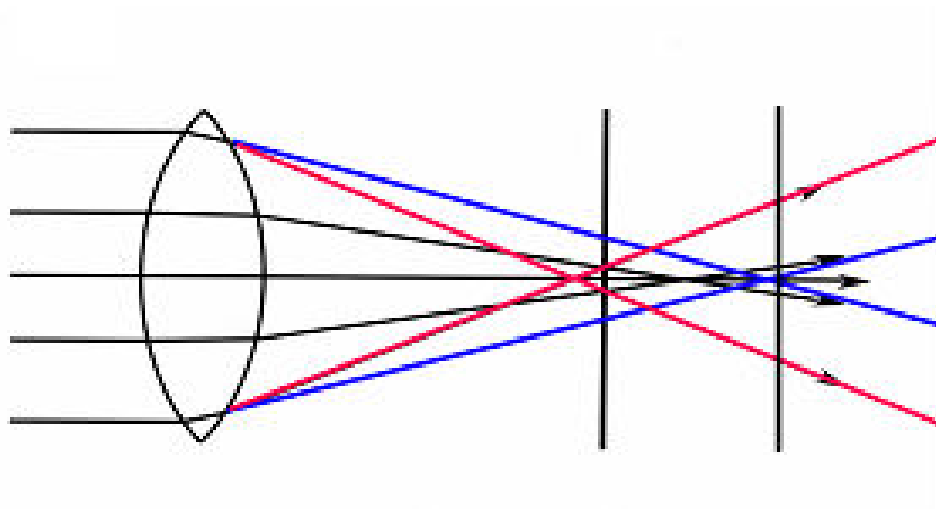
Defocus

$$\delta_f = f\alpha$$

Spherical aberration

$$\delta_s = C_s \alpha^3$$

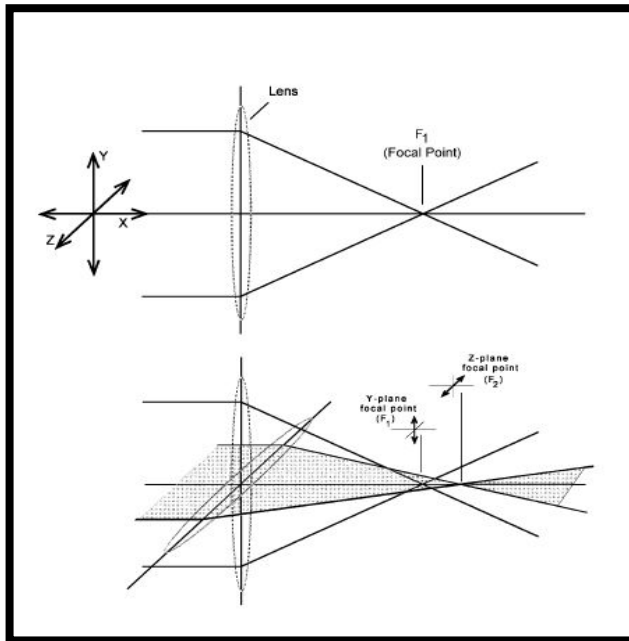
Scherzer: in a lens system with radial symmetry the spherical aberration can never be completely corrected



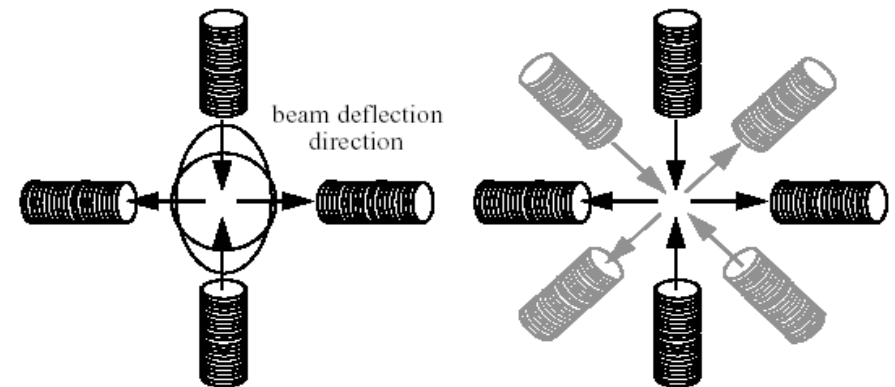
Chromatic aberration

$$\delta_c = C_c \left(\frac{\Delta E}{E} + 2 \frac{\Delta I}{I} \right)$$

Astigmatism



different gradients of the field:
different focalization in the two directions



It can be corrected

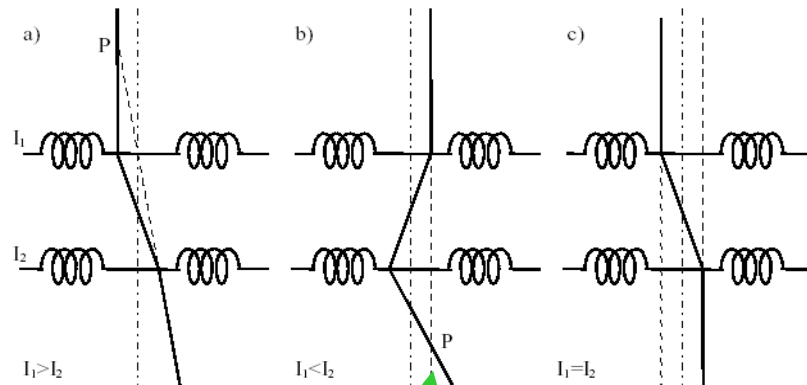
Other aberrations exist like
threefold astigmatism
Coma

...

but can be corrected or are negligible

Deflection coils

Deflection Coils

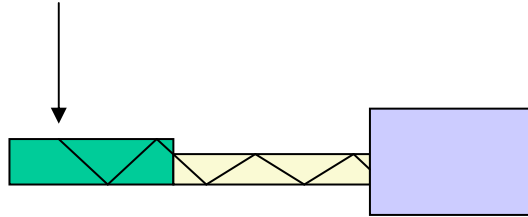


At least two series of coils are necessary to decouple the shift of the beam from its tilt

Position remains in p while different tilts are possible

Position is shifted without changing the incidence angles

Revelators



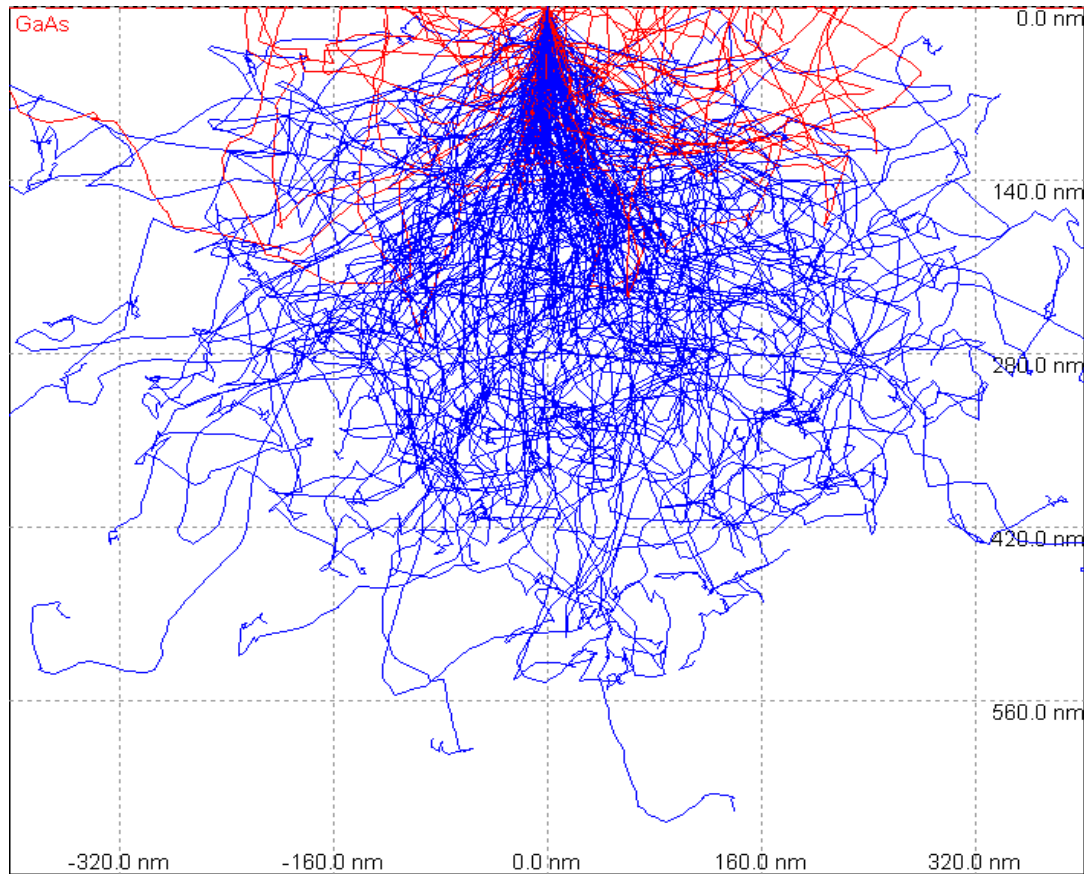
Scintillator: emits photons when hit by high-energy electrons. The emitted photons are collected by a lightguide and transported to a photomultiplier for detection.

phosphor screen: the electron excites phosphors that emit the characteristic green light



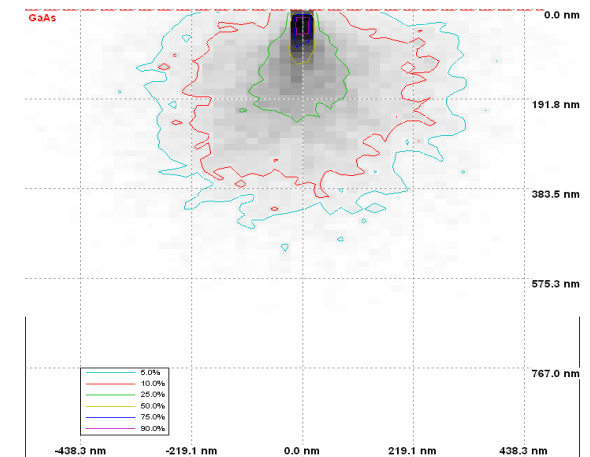
CCD conversion of charge into tension.
Initially, a small capacity is charged with respect a reference level. The load is eventually discharged. Each load corresponds to a pixel. The discharge current is proportional to the number of electrons contained in the package.

Trajectories of 10KeV electrons in matter



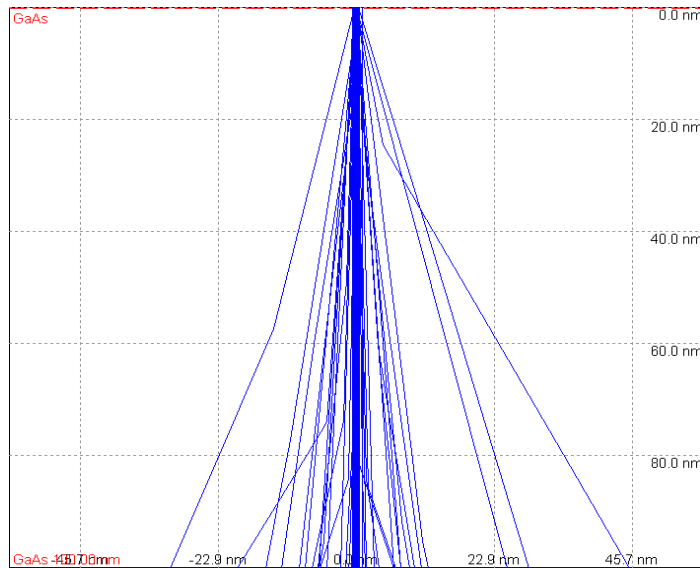
GaAs bulk

Energy released in the matrix



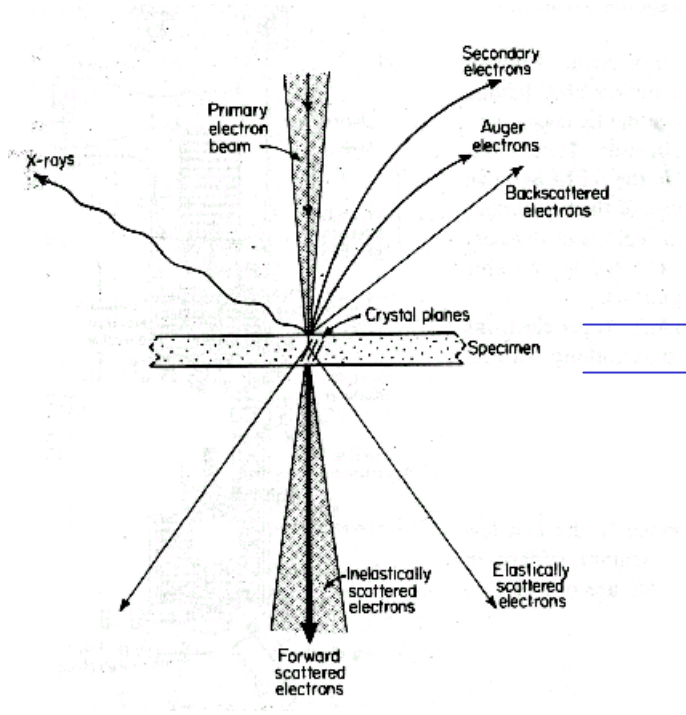
<http://www.gel.usherbrooke.ca/casino/download2.html>

Trajectories of 100KeV electron in a thin specimen



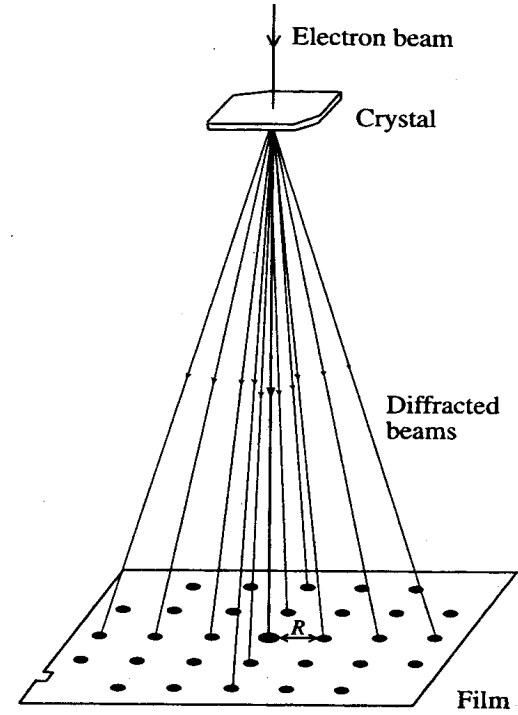
GaAs thin film

Interaction electronic beam – sample: electron diffraction



backscattering

forward scattering



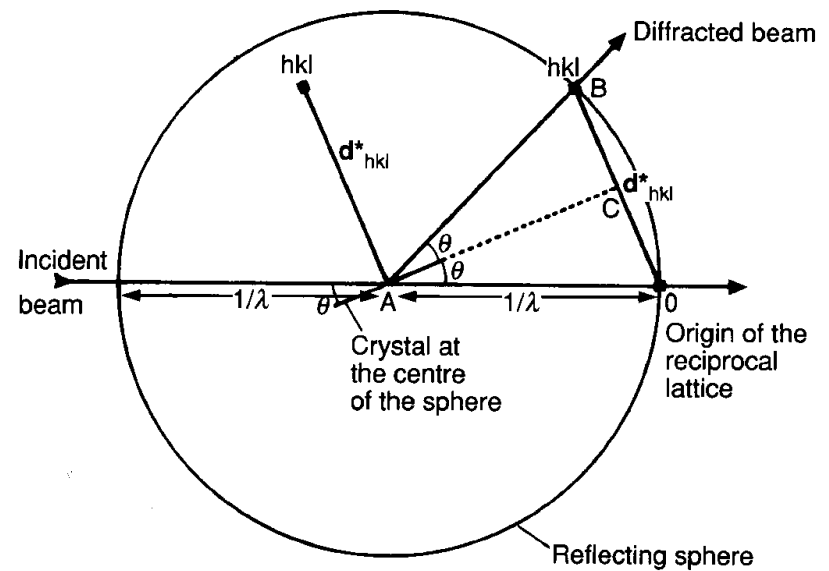
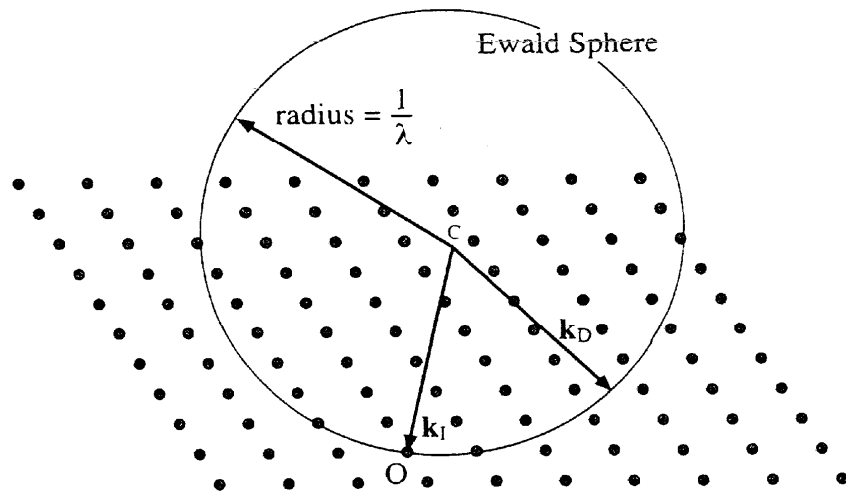
Electrons can be focused by electromagnetic lenses



The diffracted beams can be recombined to form an image

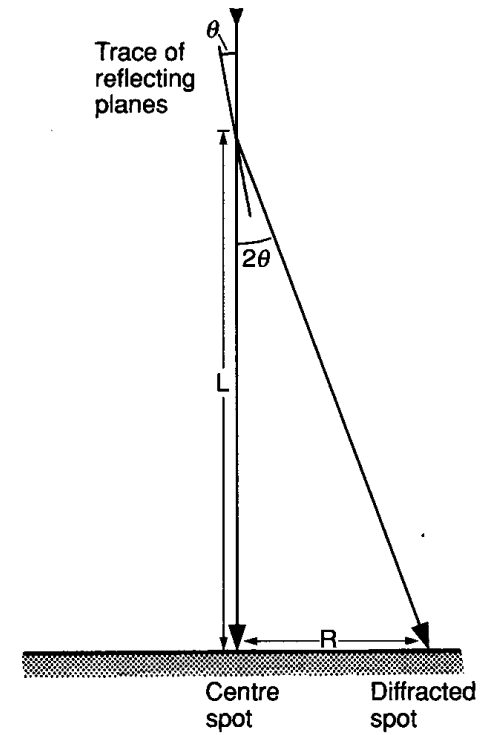
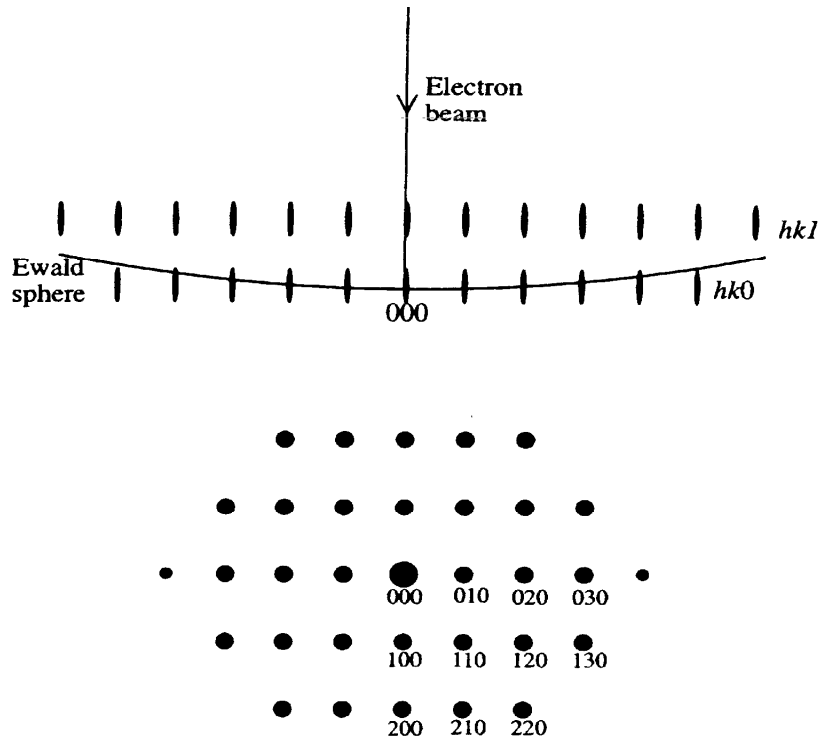
Electron diffraction - 1

Diffraction occurs when the Ewald sphere cuts a point of the reciprocal lattice



$$\text{Bragg's Law } 2d \sin \theta = \lambda$$

Electron diffraction - 2



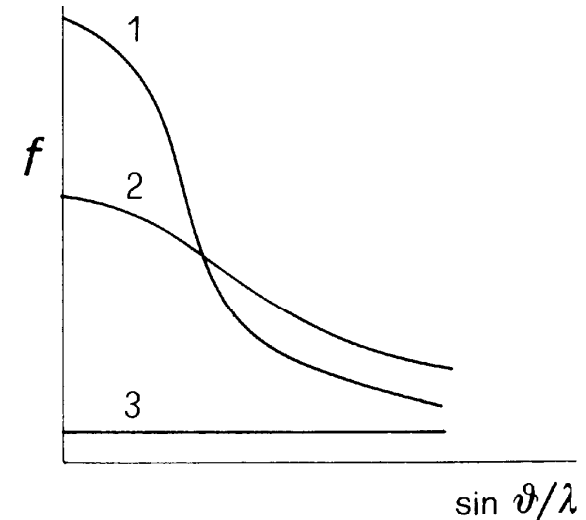
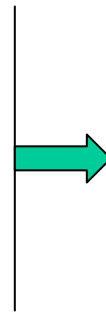
$$\frac{R}{L} = \frac{1/d}{1/\lambda} \quad \Rightarrow \quad d = \frac{\lambda L}{R}$$

Recorded spots correspond mainly to one plane in reciprocal space

Scattering

Fast electrons are scattered by the protons in the nuclei, as well as by the electrons of the atoms

X-rays are scattered only by the electrons of the atoms



Typical scattering curves for:
(1) electrons; (2) X-rays; (3) neutrons.

Diffacted intensity is concentrated in the forward direction.
Coherence is lost with growing scattering angle.

Comparison between high energy electron diffraction and X-ray diffraction

Electrons (200 kV)

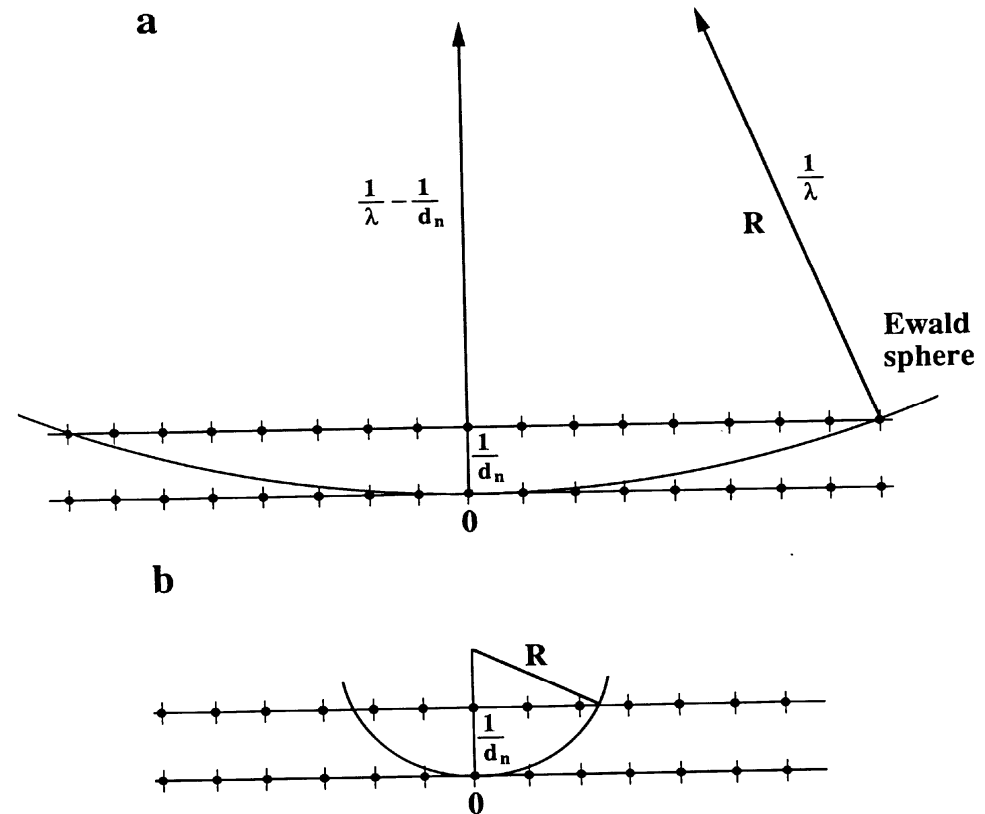
$$\lambda = 2.51 \text{ pm}$$

$$r_E = 2.0 \cdot 10^{11} \text{ m}$$

X-ray (Cu K_α)

$$\lambda = 154 \text{ pm}$$

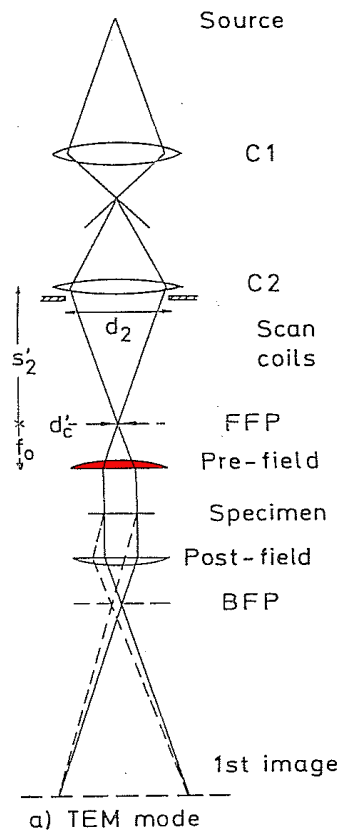
$$r_E = 3.25 \cdot 10^9 \text{ m}$$



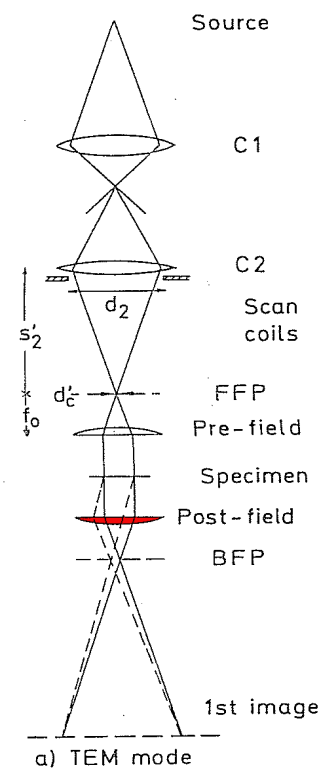
Objective lens

Objective is the most important lens in a TEM, it has a very high field (up to 2 T)

The Specimen is completely immersed in its field so that pre-field and post field can be distinguished



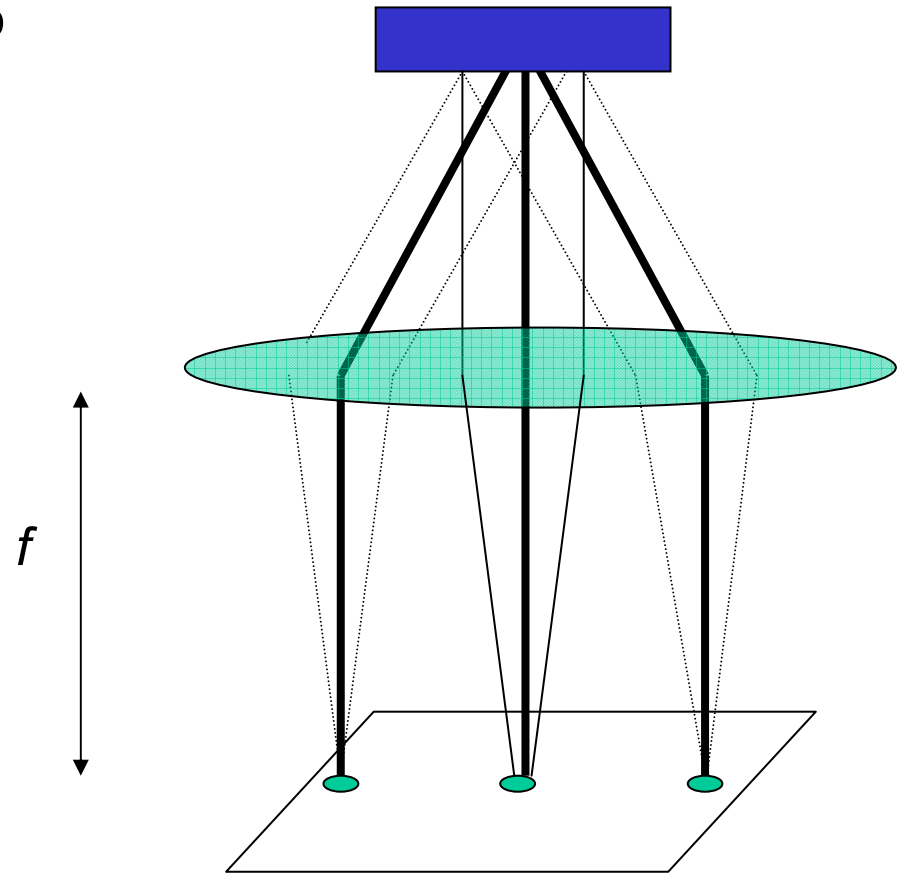
The magnetic pre-field of the objective lens can also be used to obtain a parallel illumination on the specimen



The post field is used to create image or diffraction from diffracted beams

Diffraction mode

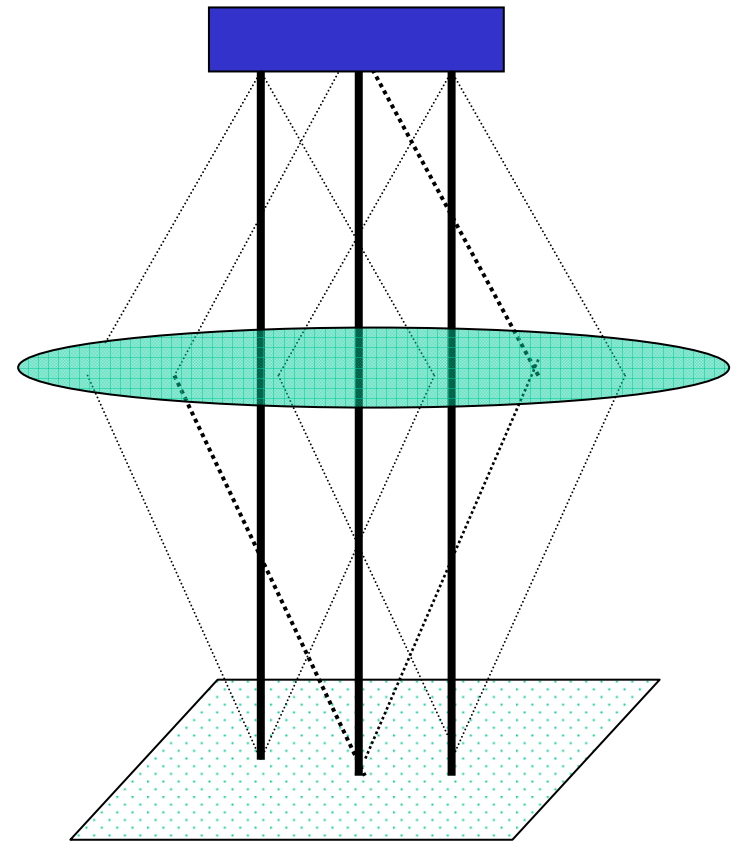
Different directions correspond to different points in the back focal plane



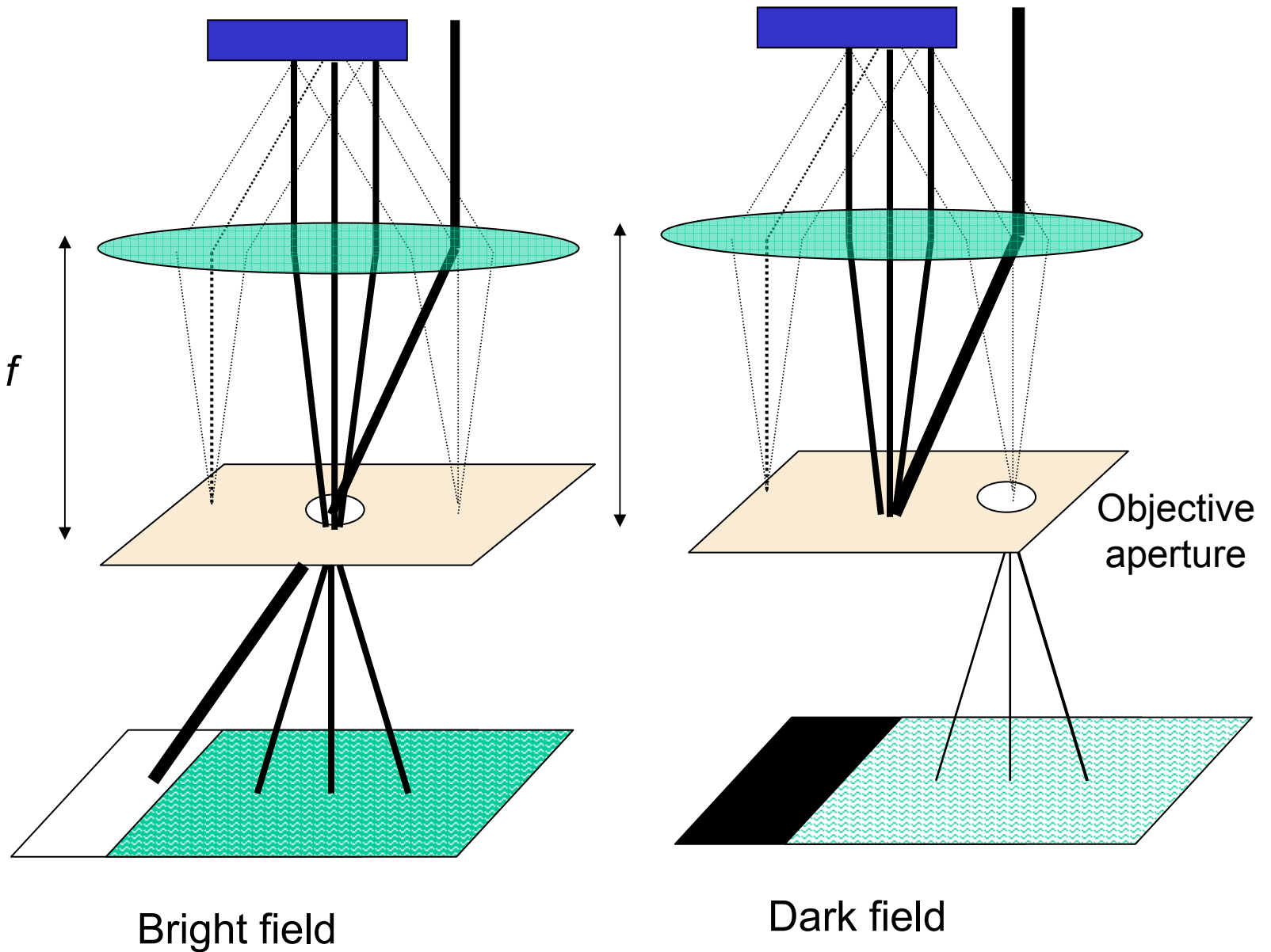
Imaging mode

Different point correspond to different points.

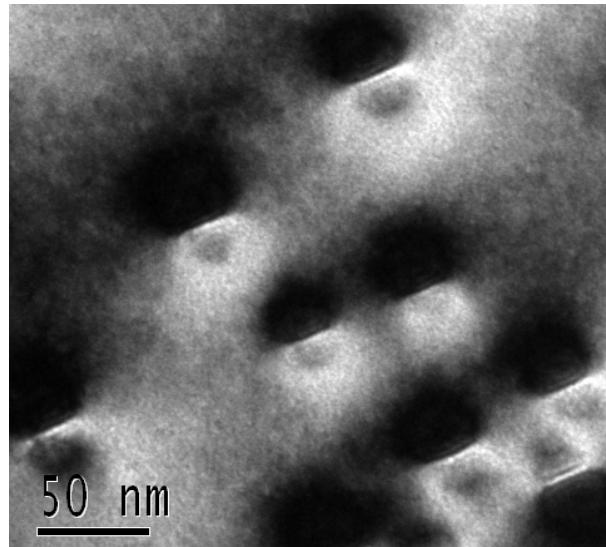
All diffraction from the same point in the sample converge to the same image in the image plane



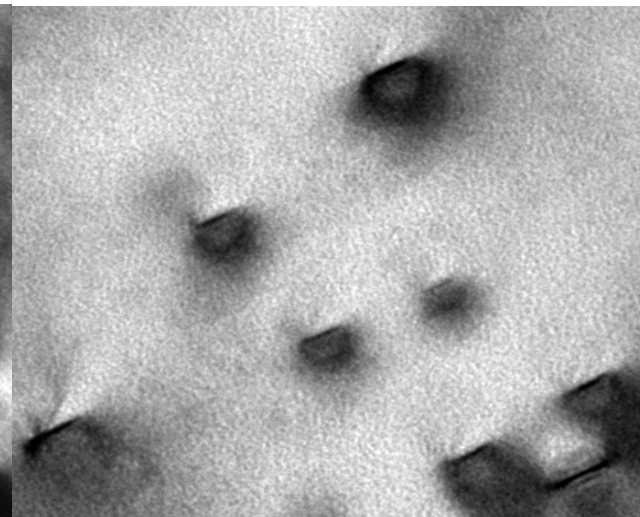
Contrast enhancement by single diffraction mode



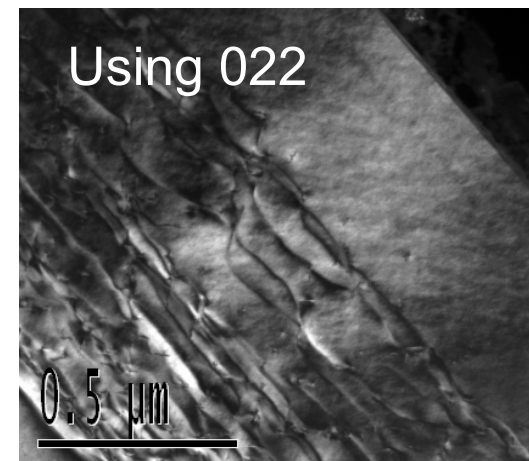
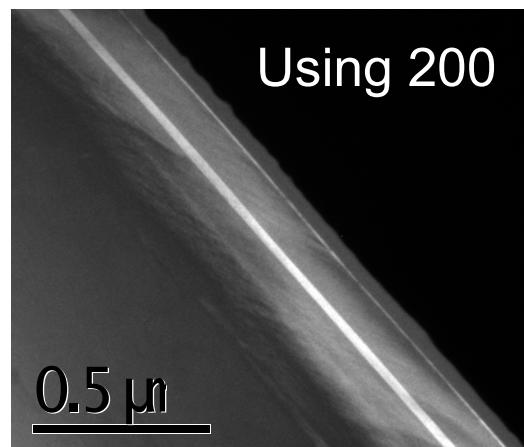
Dark/bright field images



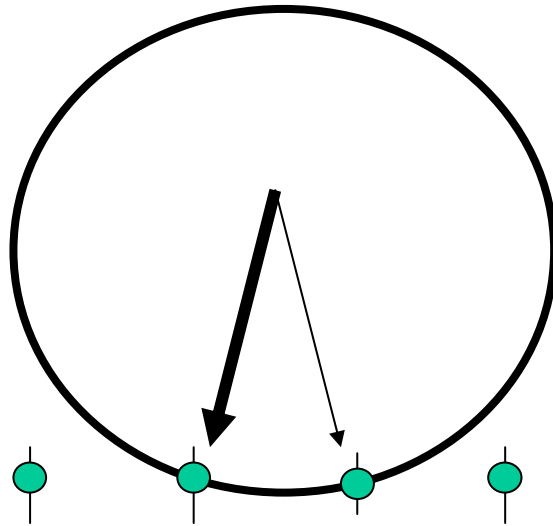
Dark field



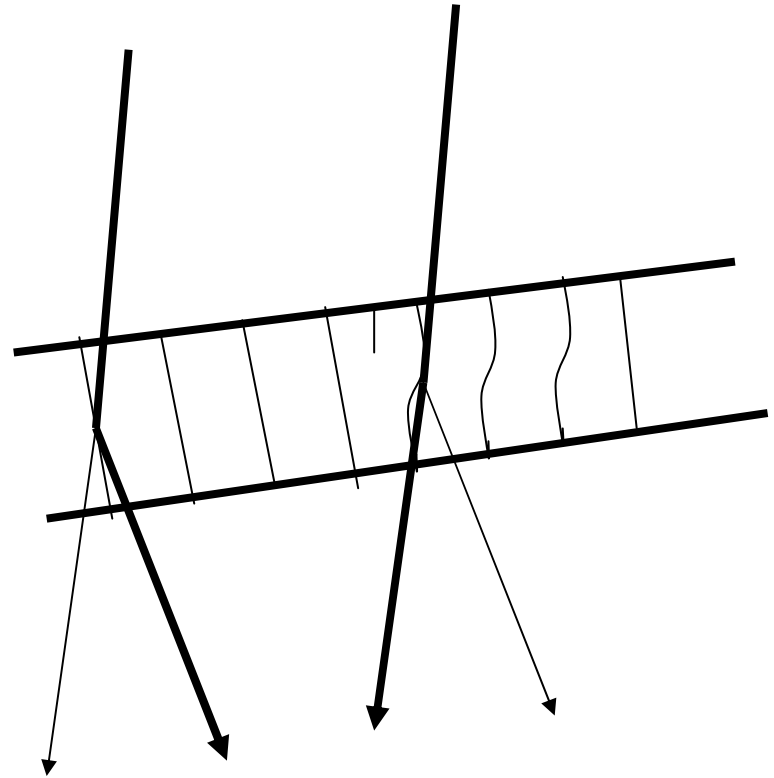
Bright field



Diffraction contrast

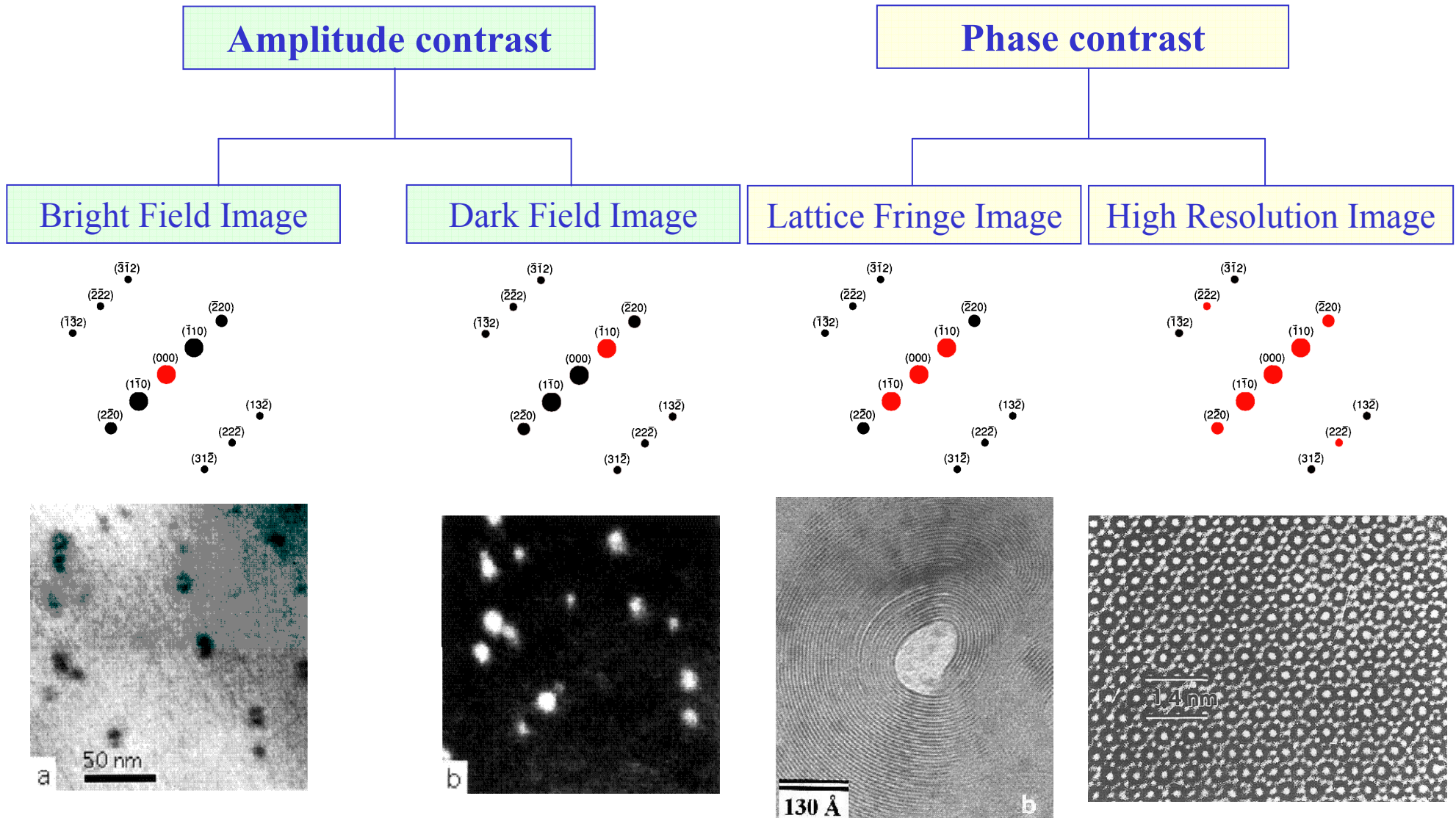


Suppose only two beams are on

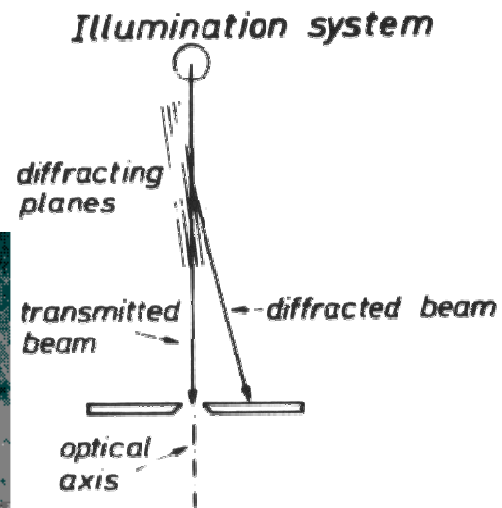
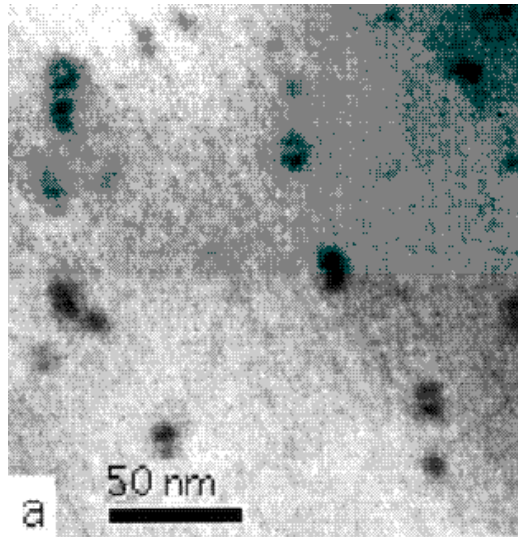


Imaging

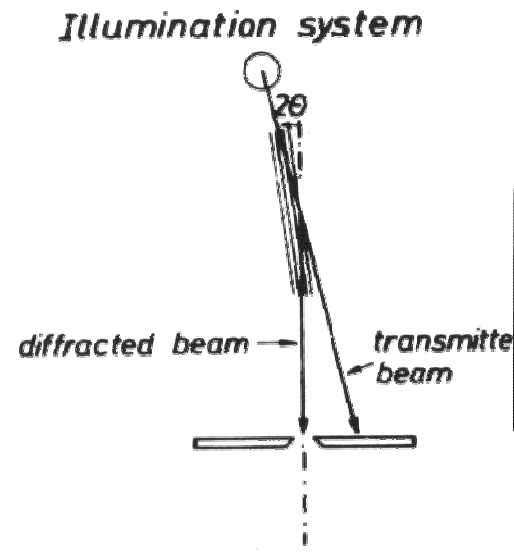
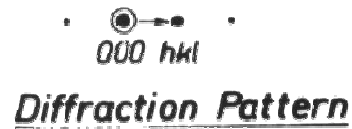
Perfect imaging would require the interference of **all** diffraction channels. Contrast may however be more important.



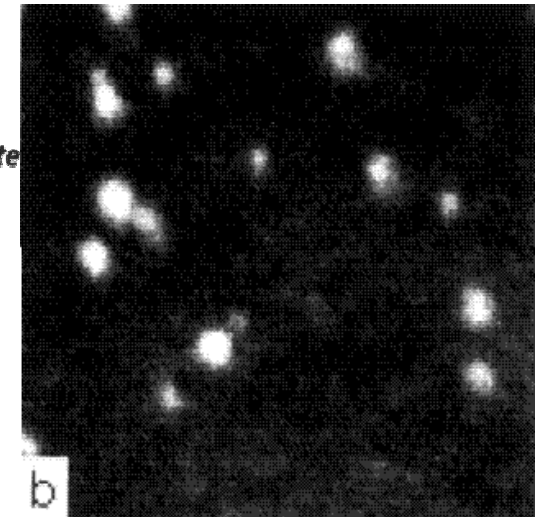
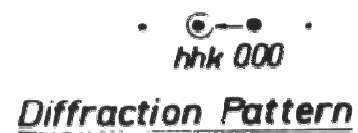
Amplitude contrast - 1



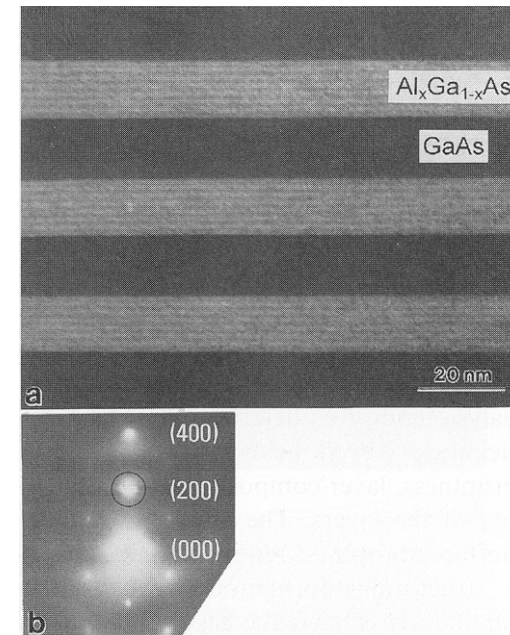
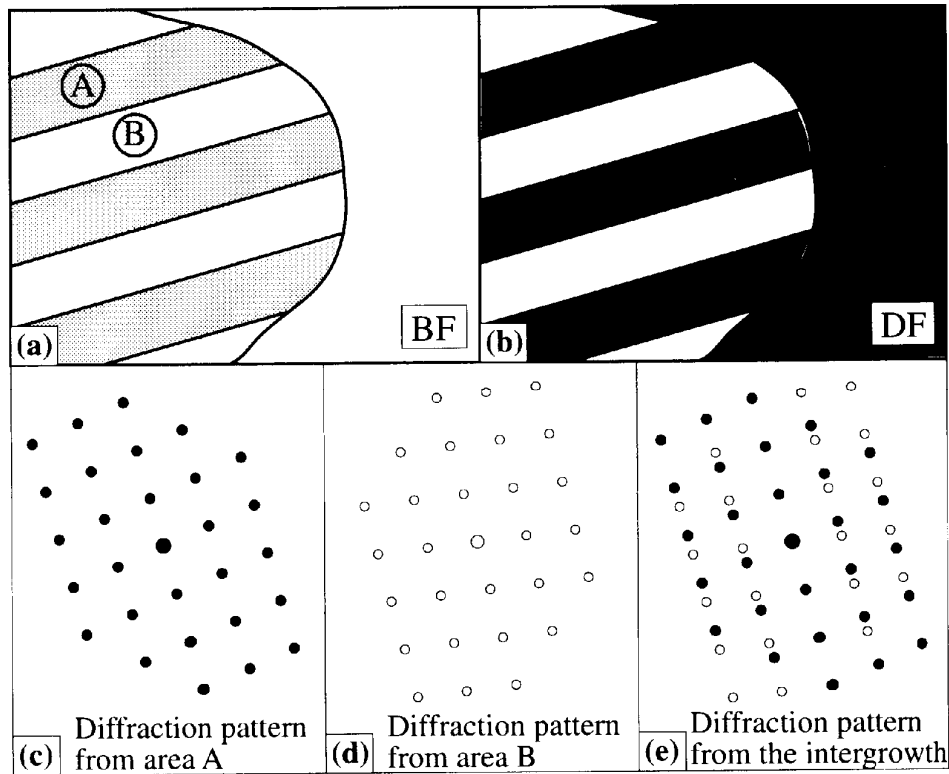
Bright Field



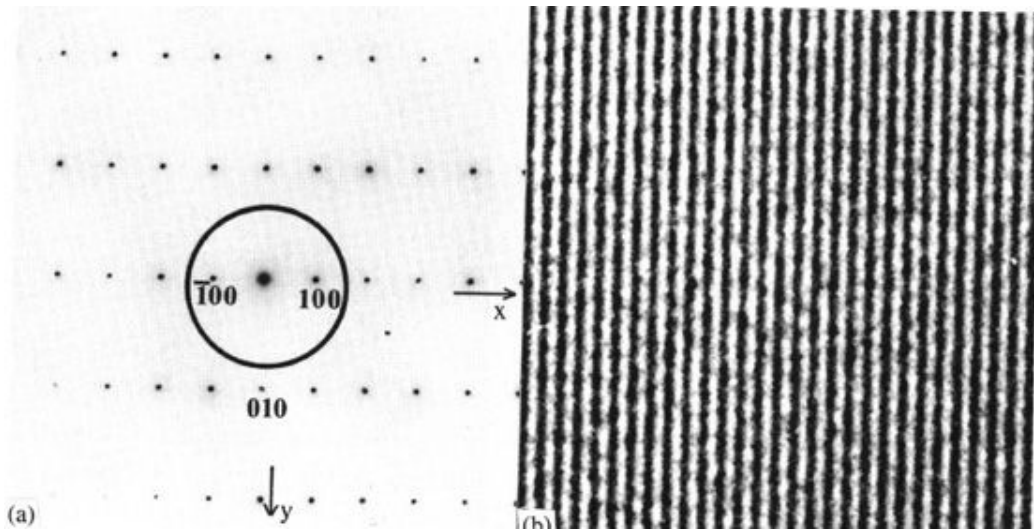
Dark Field



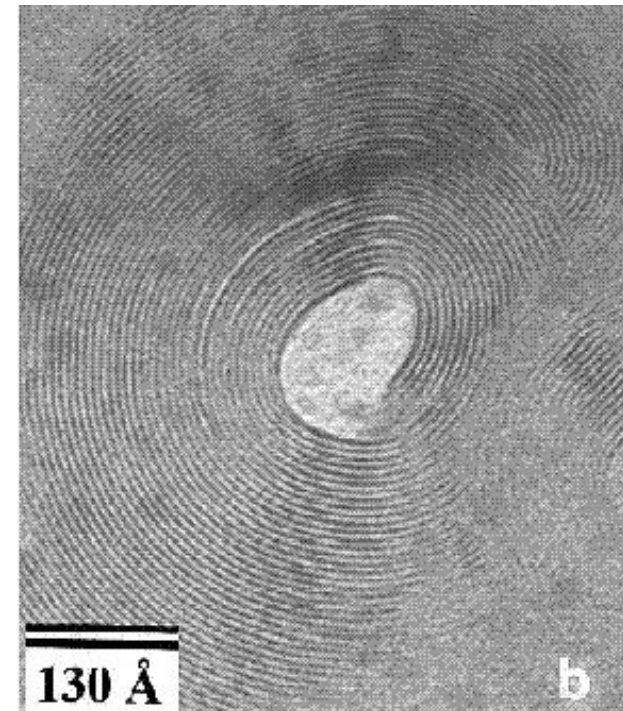
Amplitude contrast - 2



Phase contrast in electron microscopy



Fringes indicate two Dim. periodicity



Phase contrast in electron microscopy

What happens if we consider all beams impinging on the same point ? **Interference !!!**

$$|\phi_i|^2 = \left| \sum_{BEAMS} \Psi_g \right|^2$$

g a vector of the reciprocal lattice

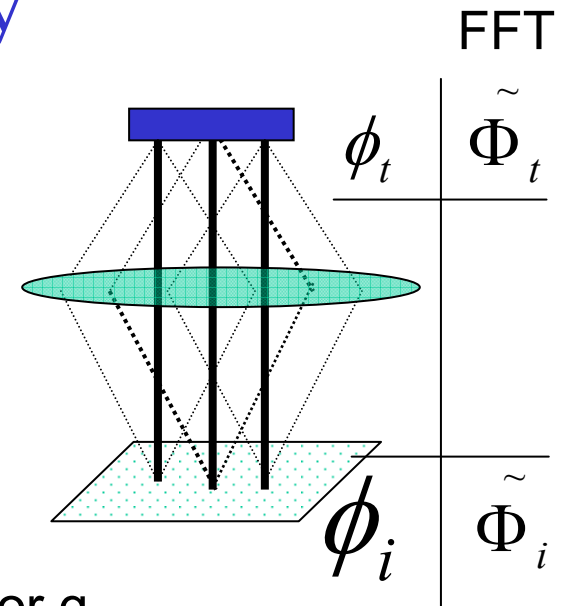
Ψ_g is the component beam scattered by a vector g

But notice that Ψ_g is the Fourier component of the exit wavefunction

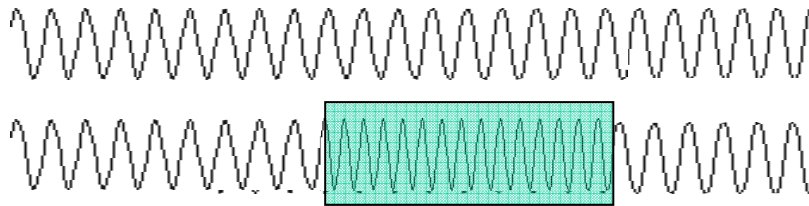
$$\sum_{BEAMS} |\Psi_g|^2 = 1$$

Indeed each electron has a certain probability to go in the transmitted or diffracted beam. For an amorphous material all Fourier components are possible but in a crystal only beams with the lattice periodicity are allowed, these are the diffracted beams.

NOTE: the diffraction pattern is just the Fourier transform of the exit wave

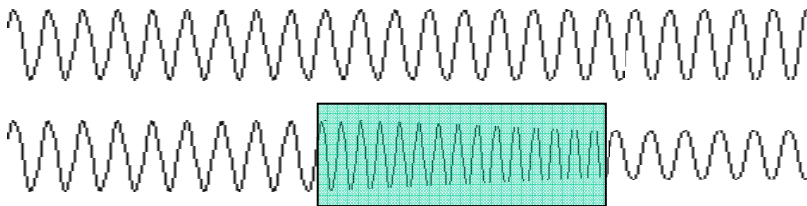


Effect of the sample potential V



Phase shift $\phi_t = e^{i\theta}$

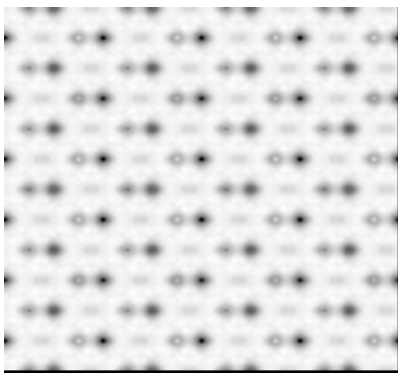
$$\phi_t \approx e^{i\sigma V} \approx 1 + i\sigma V$$



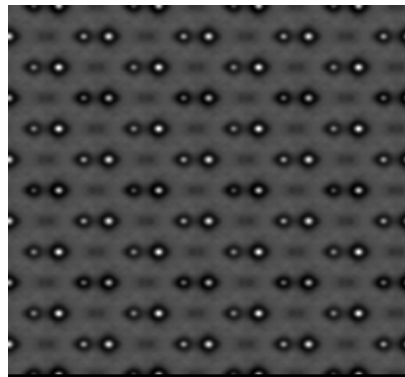
Amplitude variation $\phi_t = e^{-\mu t}$

Example of exit wave function (simulation)

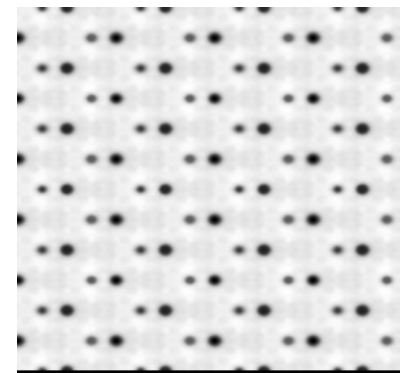
Real part



Modulus



phase



Optical Phase Contrast microscope

(useful for biological specimen which absorb little radiation but have different diffraction index with respect to surrounding medium, thus inducing a phase shift)

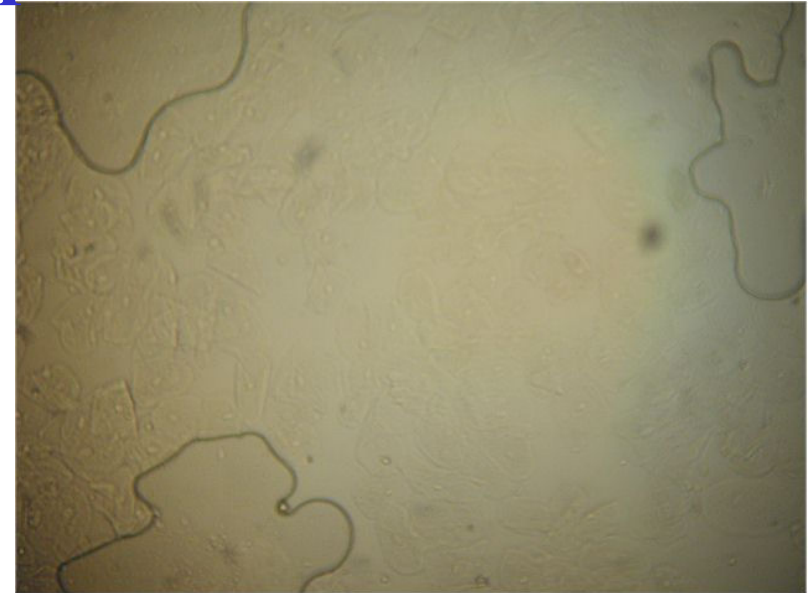
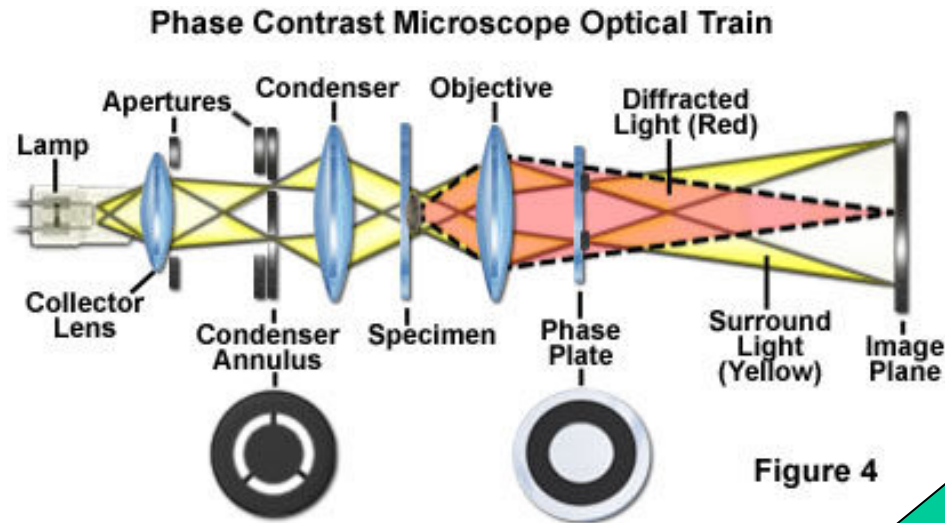
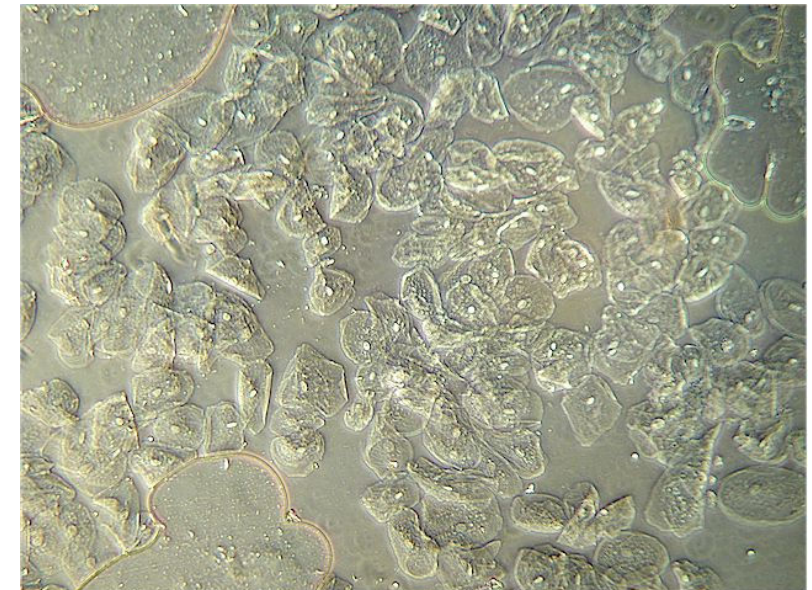


Image for regular brightfield objectives. Notice the air bubbles at three locations, some cells are visible at the left side

Same image with phase contrast objectives. White dots inside each cell are the nuclei.

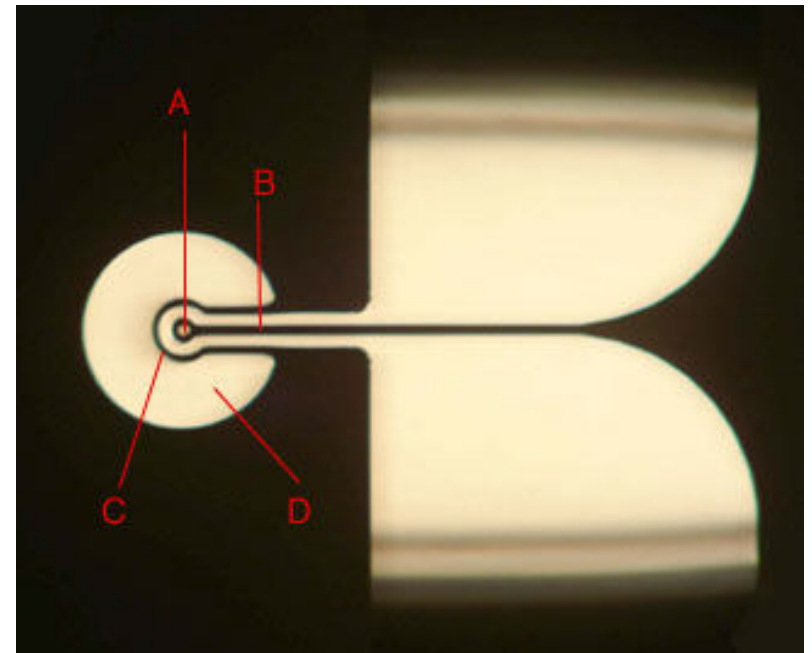


Phase contrast in electron microscopy

To build an **ideal phase microscope** we must dephase (by $\pi/2$) all diffracted beams while leaving the transmitted unchanged

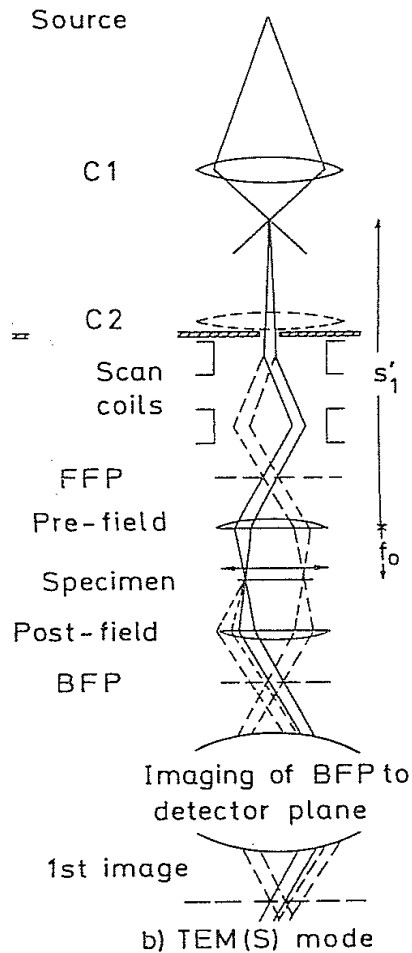
Phase adjustment device

The device is $\sim 150 \mu$ wide and 30μ thick. The unscattered electron beam passes through a drift tube A and is phase-shifted by the electrostatic potential on tube/support B. Scattered electrons passing through space D are protected from the voltage by grounded tube C.

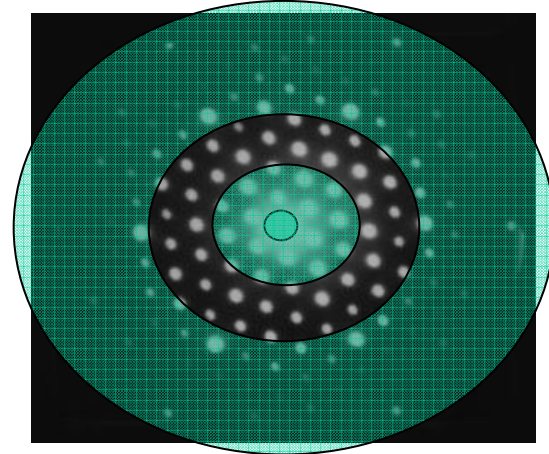


STEM

An alternative use of the electron microscope is to concentrate the electron beam onto a small area and scan it over the sample. Initially it was developed to gain local chemical information. Actually structural information can be gained, too, since the beam spot can be as small as 1.3 Å.



Diffraction mode



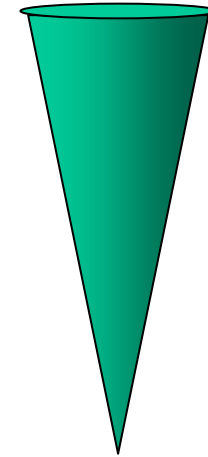
While scanning the beam over the different part of the sample we integrate over different diffraction patterns. If the transmitted beam is included the method is called STEM-BF otherwise STEM-DF

The dark field image corresponds to less coherent electrons and allows therefore for a more accurate reconstruction

STEM probe

It depends on
aperture , Cs , defocus

$$P^2(\vec{r}_{probe} - \vec{r}, 0, \Delta) = \left| \int_{|\vec{K}|=0}^{|\vec{K}|_{\max}} e^{-i\chi(\vec{k})} e^{i\vec{k}(\vec{r}_{probe} - \vec{r})} d^2\vec{k} \right|^2$$



It is the sum of the waves at different angles, each with its own phase factor.

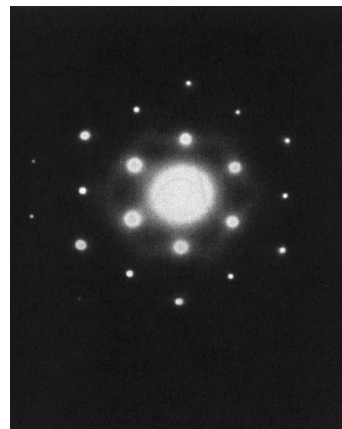
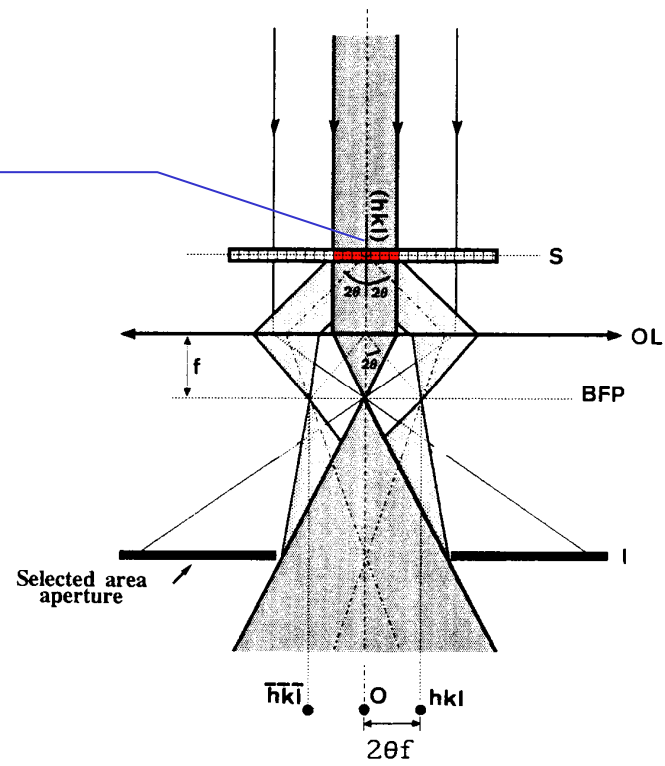
If there is no aberration the larger is the convergence, the smaller is the probe.

The presence of aberrations limits the maximum value of the convergence angle up to 14 mrad

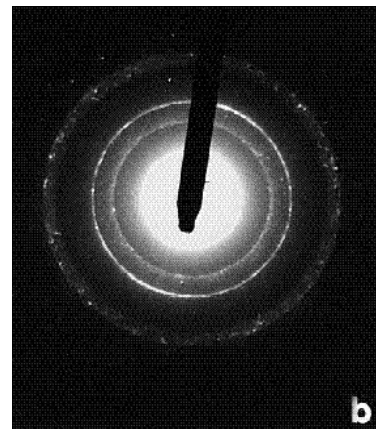
The different wavevectors contributing to the incoming wave blur up the diffraction pattern, causing superposition of the spots. Interference effects are unwanted and smallest at the largest angles

Selected area electron diffraction - SAED

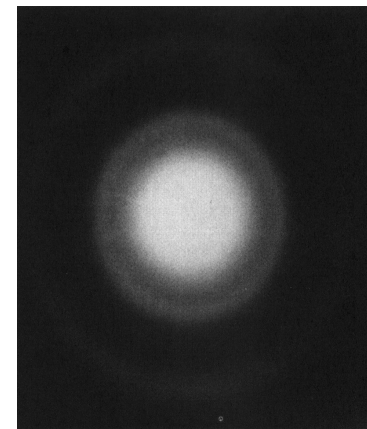
The diffracting area is $\sim 0.5 \mu\text{m}$ in diameter



Single crystal



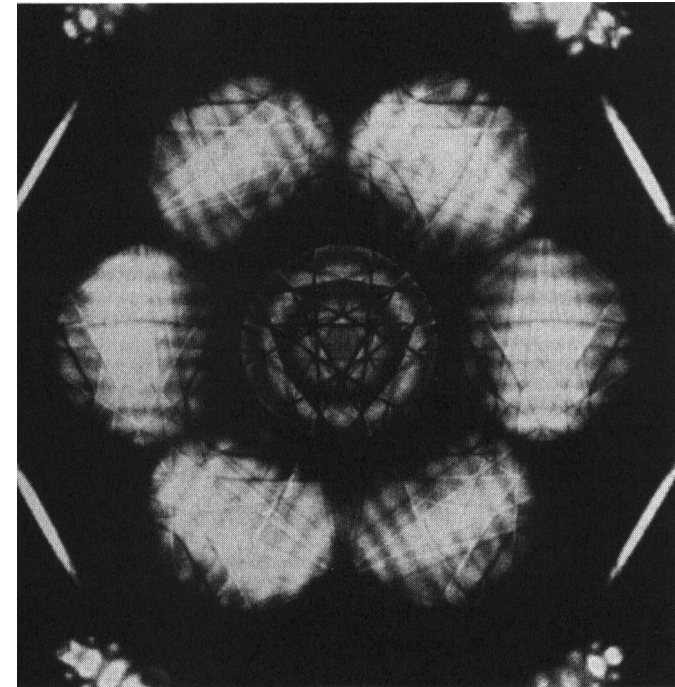
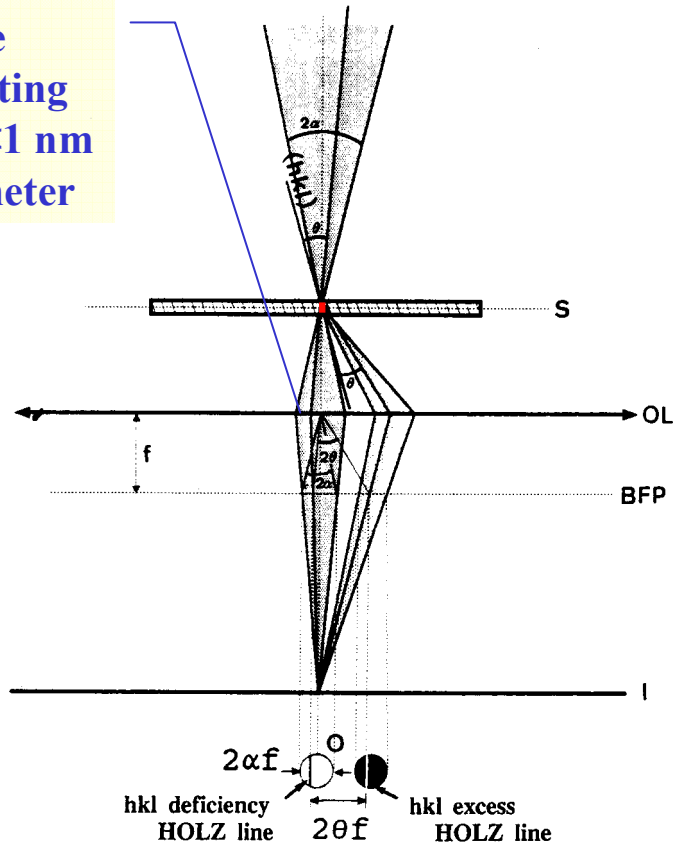
Polycrystalline



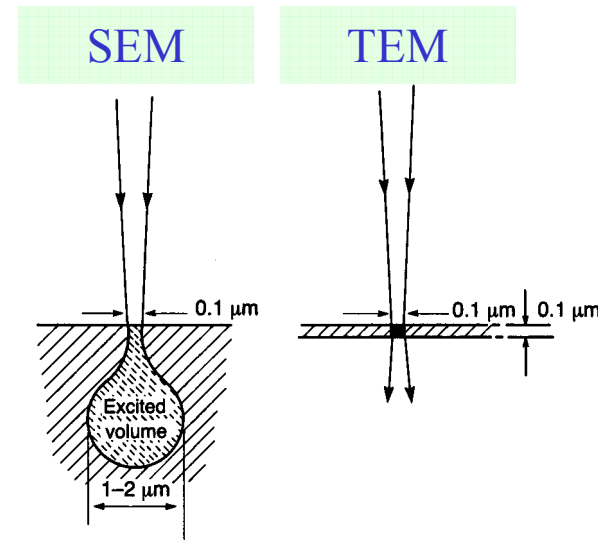
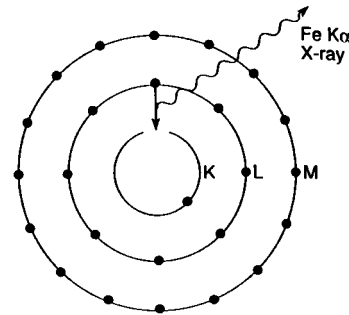
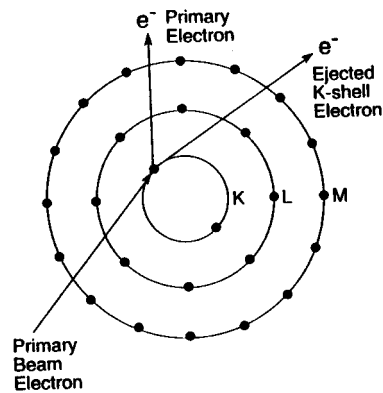
Amorphous

Convergent beam electron diffraction - CBED

The diffracting area is <1 nm in diameter



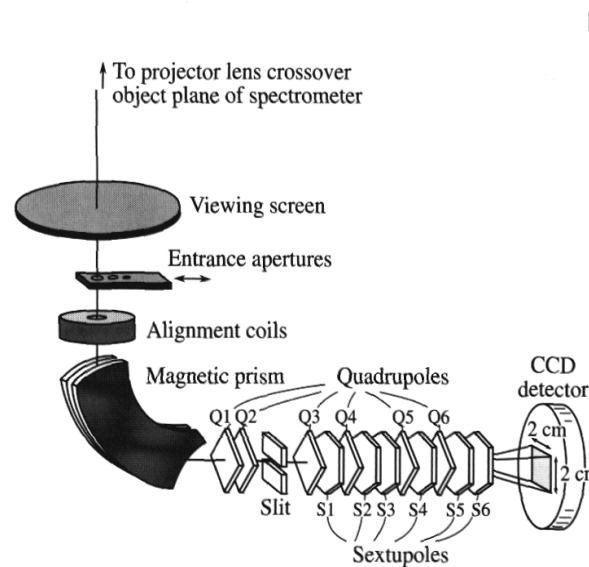
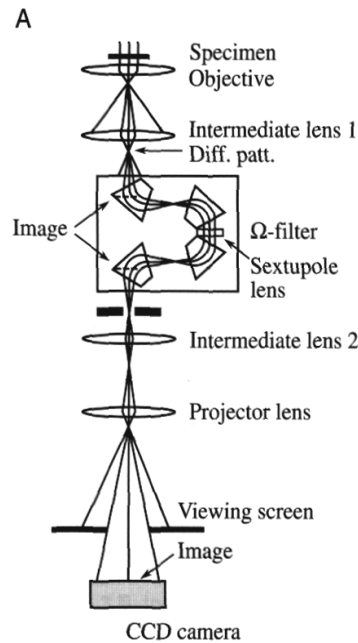
Chemical analysis: energy dispersive spectrometry



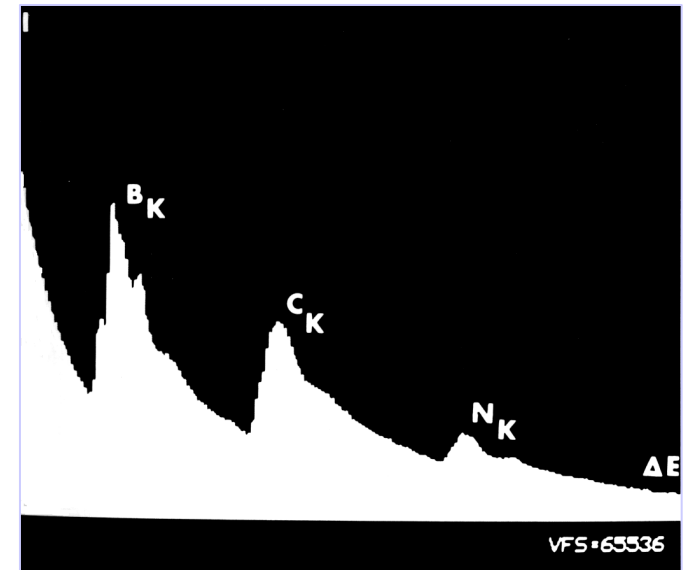
The electron beam can be focused to obtain a spot less than 500 nm

EELS

Used to collect spectra and images



Usable in both
scanning and tem
mode

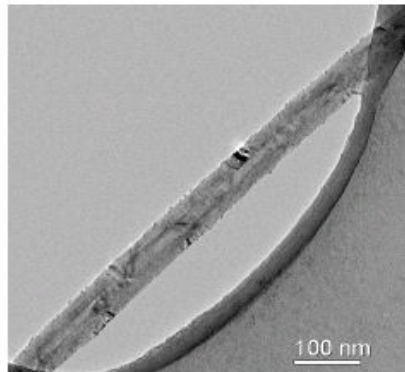


Each edge is characteristic for each material

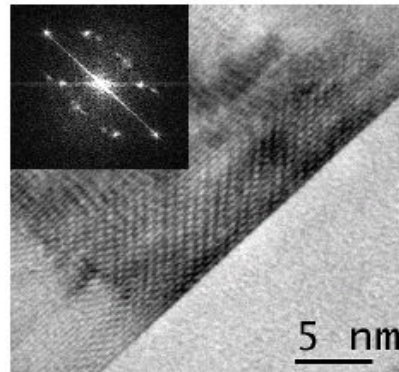
The fine structures of the edge reveal the characteristics of the local environment of the species. If the relevant inelastic event corresponds to a localized interatomic transition, the information is local, too

EELS analysis

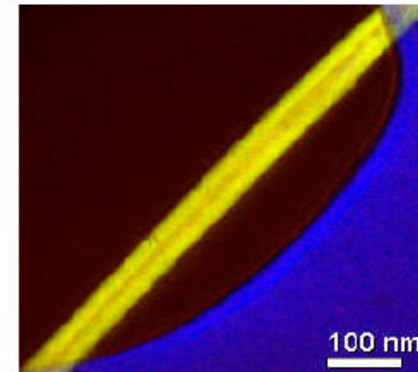
Structural and compositional characterization of nanostructures with EFTEM (Energy Filtered Transmission Electron Microscopy)



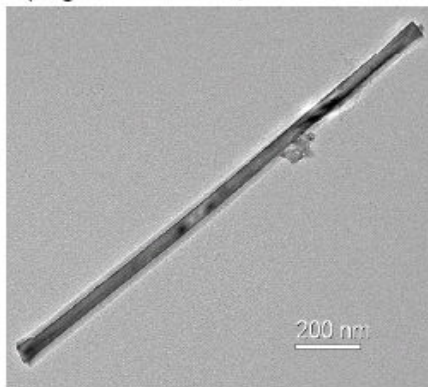
TEM image of BoronNitride nanotube
(magnification ~x100,000)



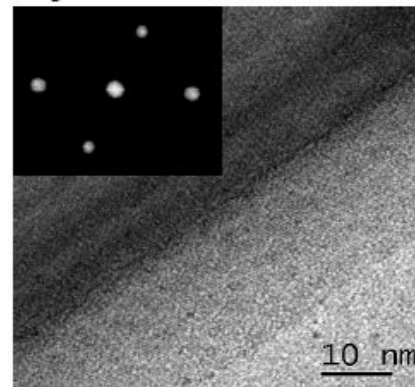
HRTEM image of BN nanotube.
Insert is the diffraction (FFT) pattern
Magnification ~x 2,000,000



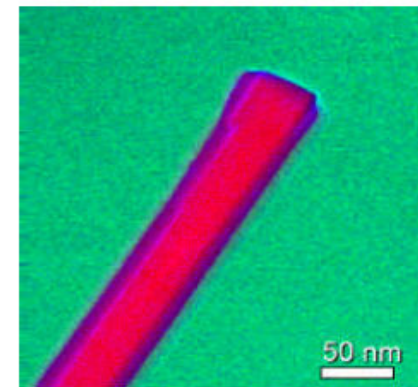
Map of elemental composition made with
GIF: Carbon-blue, BoronNitride-yellow



TEM image of Boron whisker
Magnification~x50,000



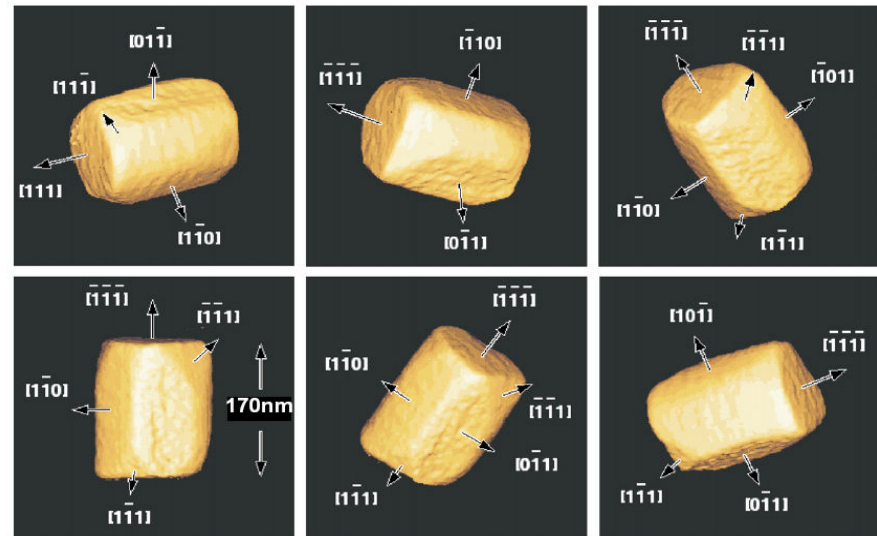
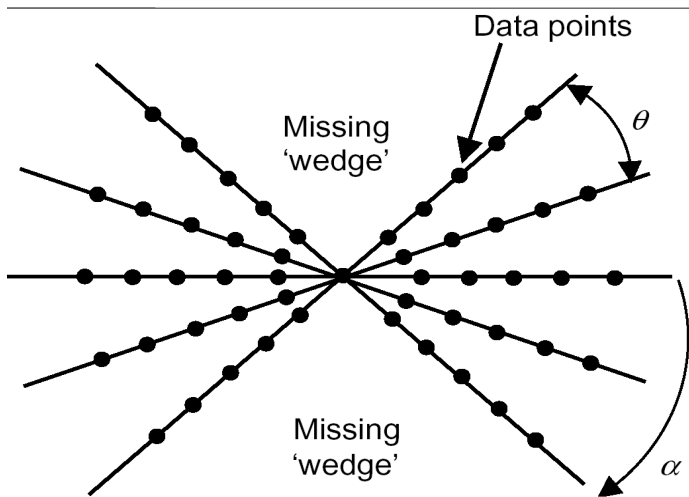
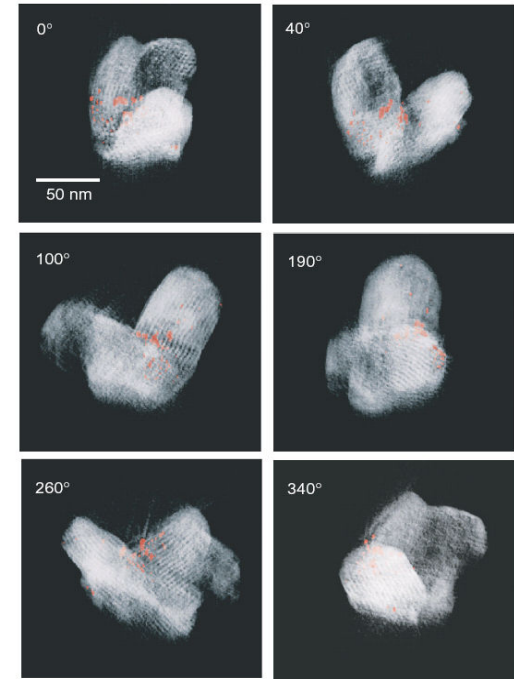
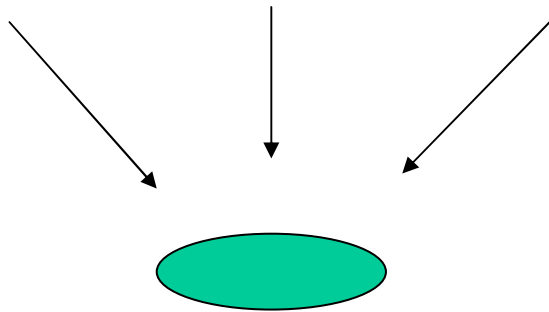
HRTEM image of Boron whisker. Insert is the diffraction
(FFT) pattern, magnification ~1,000,000



Map of elemental composition made with
GIF: Boron red;Silicon-green;Oxygen-blue

Tomography

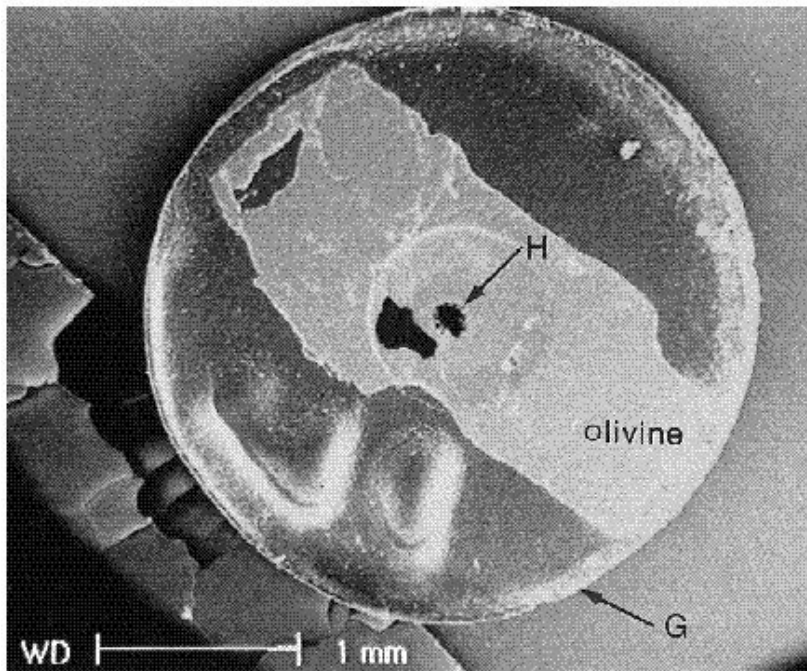
By observing at different angle it is possible to reconstruct the 3D image



Drawback of TEM: necessity of sample preparation

Milling

Ion milling



Hand milling

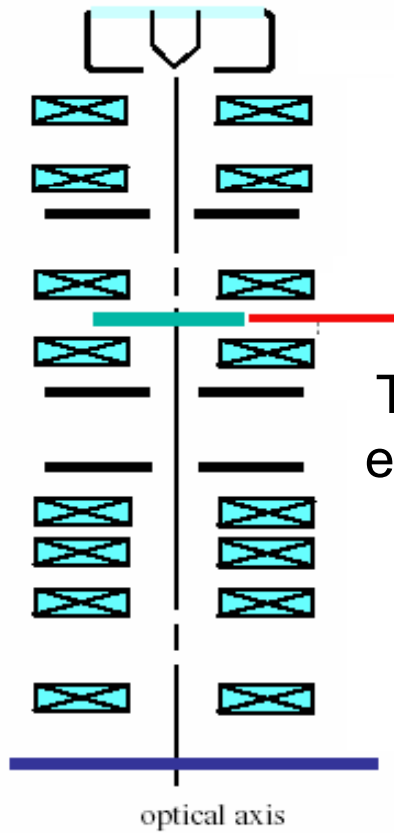


Powders

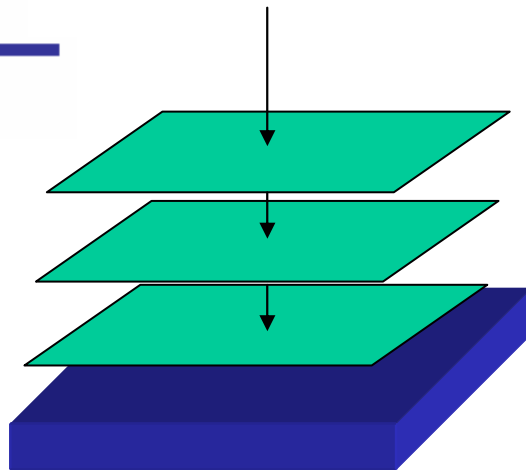
TEM DEVELOPMENTS

- An additional class of these instruments is the **electron cryomicroscope**, which includes a specimen stage capable of maintaining the specimen at liquid nitrogen or liquid helium temperatures. This allows imaging specimens prepared in vitreous ice, the preferred preparation technique for imaging individual molecules or macromolecular assemblies.
- In analytical TEMs the elemental composition of the specimen can be determined by analysing its X-ray spectrum or the energy-loss spectrum of the transmitted electrons.
- Modern research TEMs may include aberration correctors, to reduce the amount of distortion in the image, allowing information on features on the scale of 0.1 nm to be obtained (resolutions down to 0.08 nm have been demonstrated, so far). Monochromators may also be used which reduce the energy spread of the incident electron beam to less than 0.15 eV.

Other Electron Microscopes

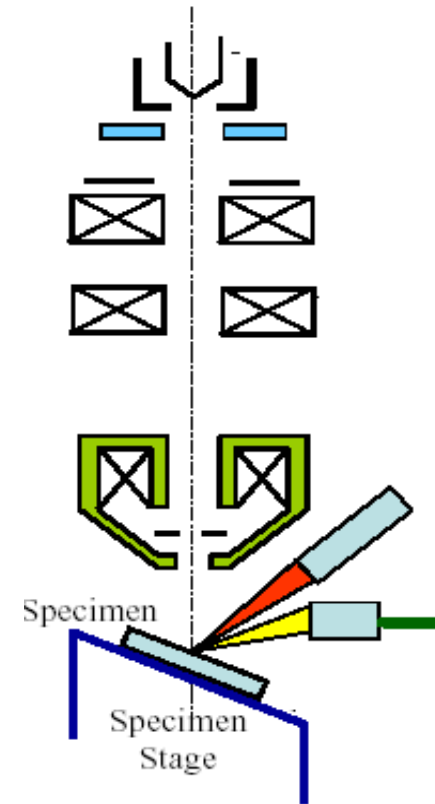
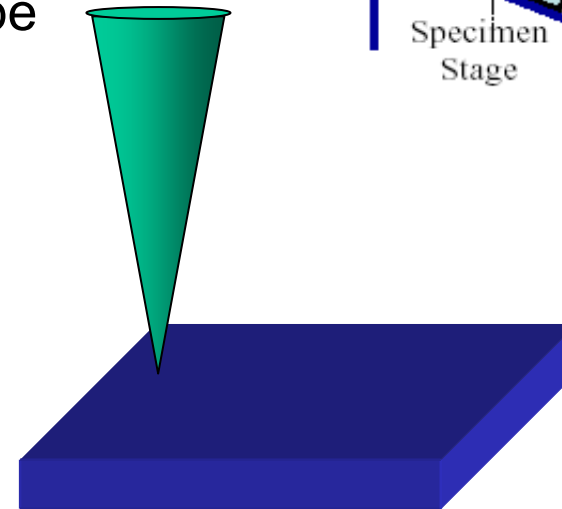


TEM : transmission
electron microscope

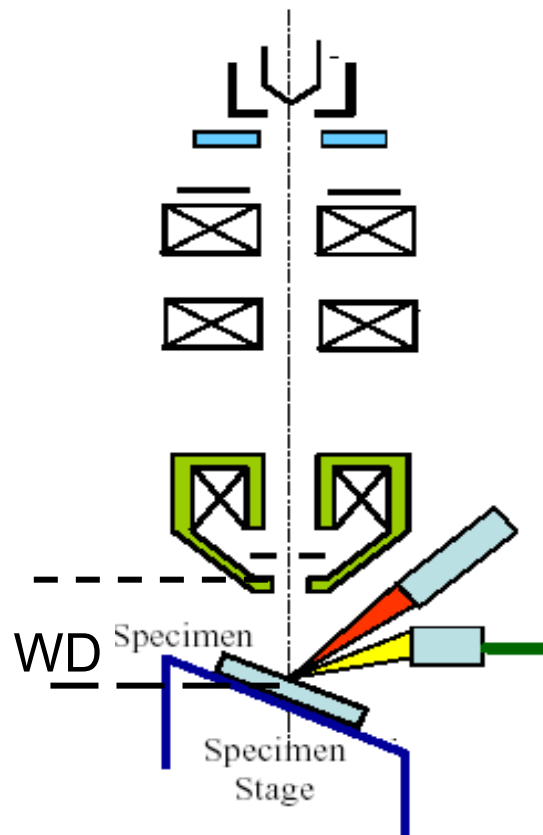


SEM : scanning electron
microscope

STEM: scanning
transmission electron
microscope



SEM



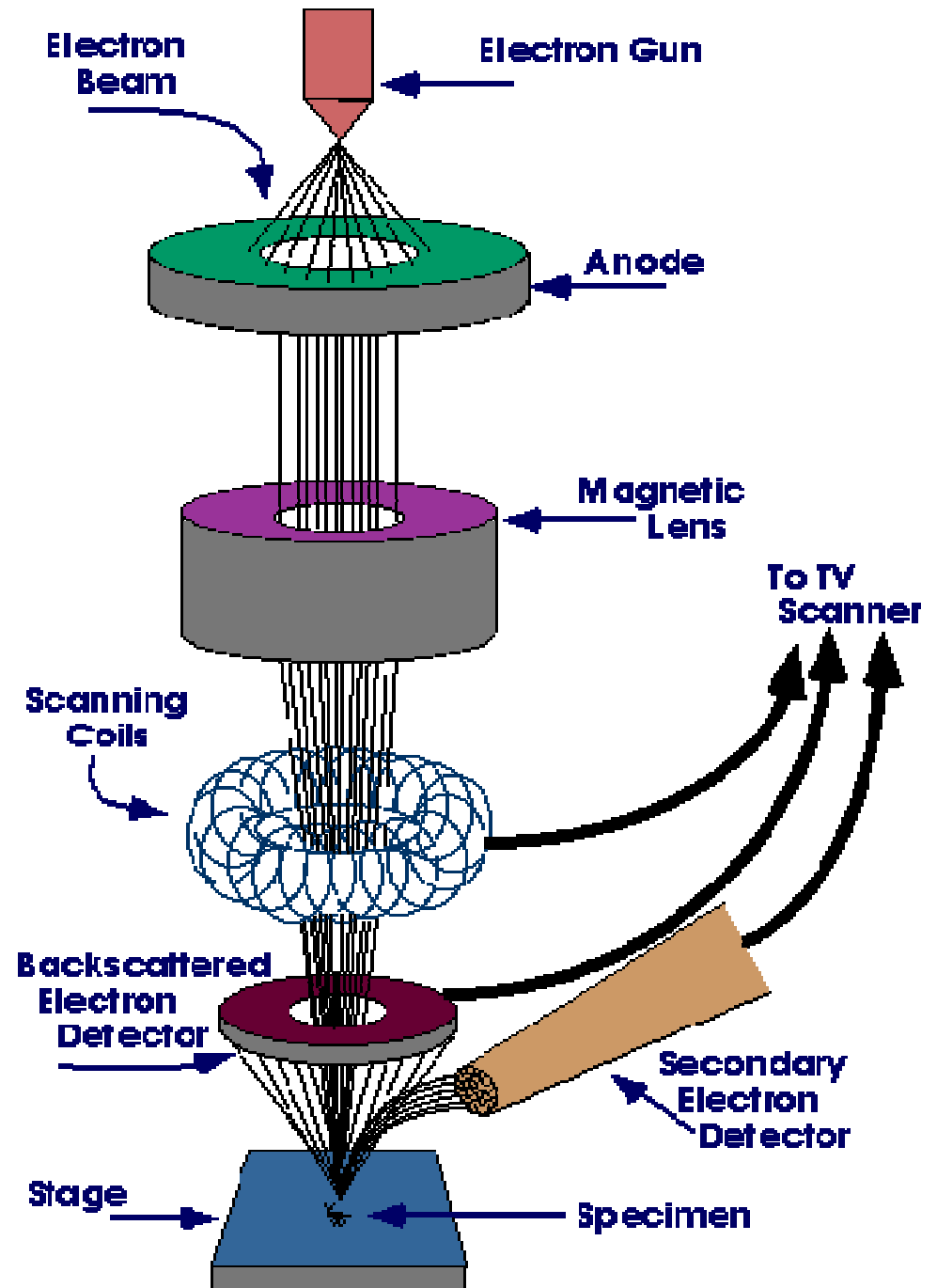
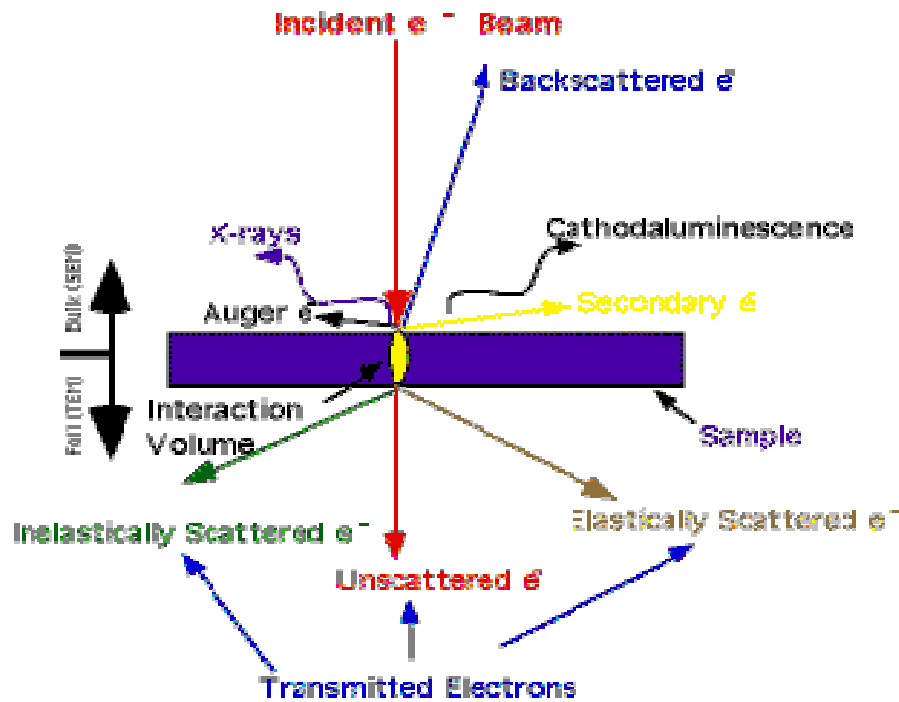
The signal arises from secondary electrons ejected by the sample and captured by the field of the detector

It is equivalent to the first part of the TEM but there are important differences:

- The sample is outside the objective lens.
- The signal recorded corresponds to reflected or to secondary electrons.
- No necessity for difficult sample preparation
- Max resolution 2 nm

The distance of the sample is called **working distance WD**

SEM

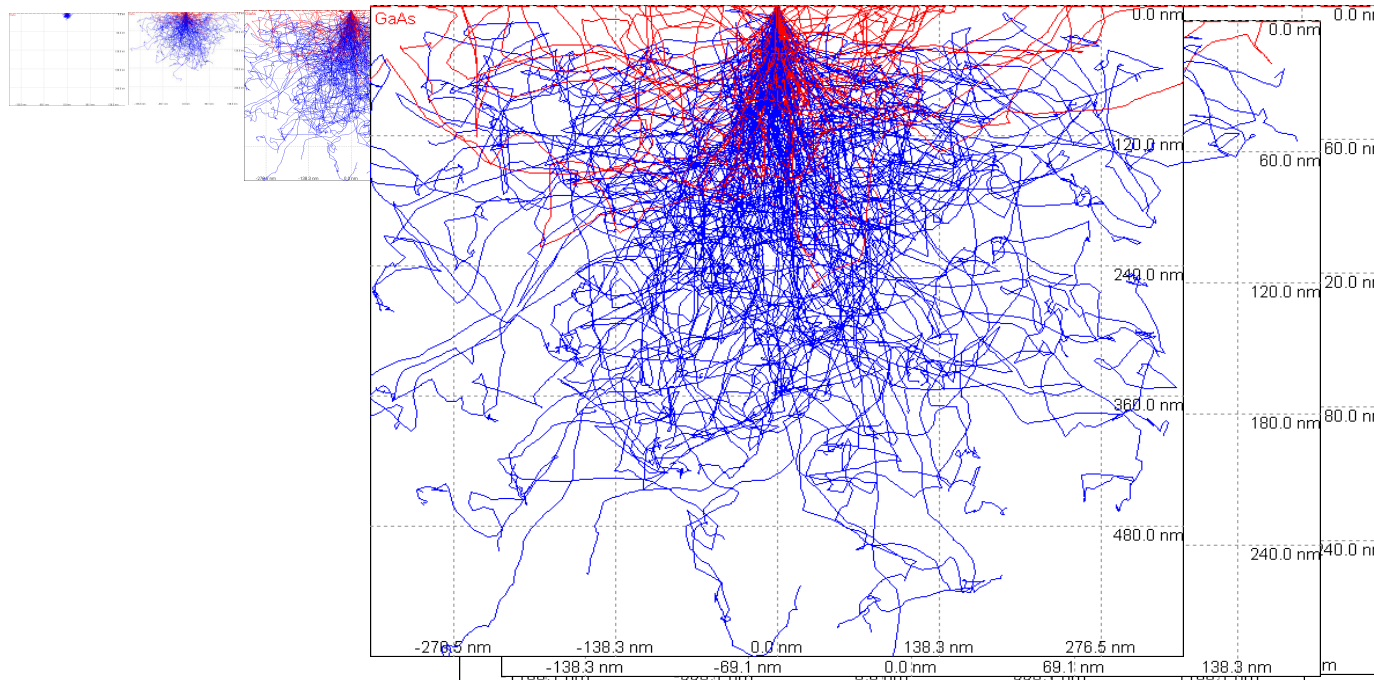


Range vs accelerating voltage

$$R = (0.052 / \rho) E_{beam}^{1.75}$$

Range of electrons in a material

$$g(z) = \frac{1}{R} \left(0.6 + 6.21 \frac{z}{R} - 12.4 \left(\frac{z}{R} \right)^2 + 5.69 \left(\frac{z}{R} \right)^3 \right)$$



Accelerating voltage

Higher voltage -> smaller probe
But larger generation pear

Higher voltage -> more backscattering

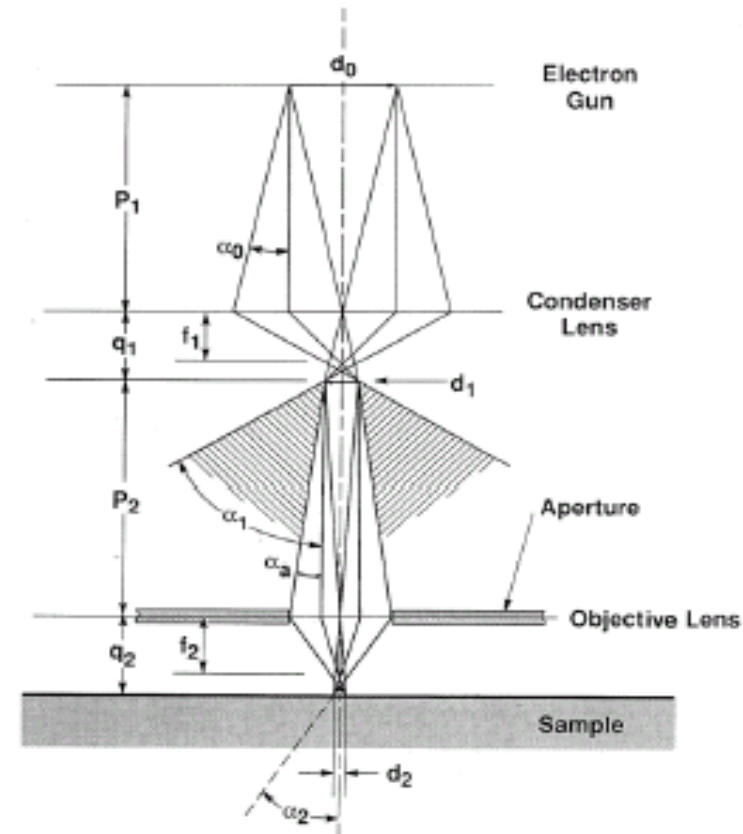
Low energy -> surface effects

Low energy (for bulk) -> lower charging

High energy (for thin sample) -> less charging

Effect of apertures

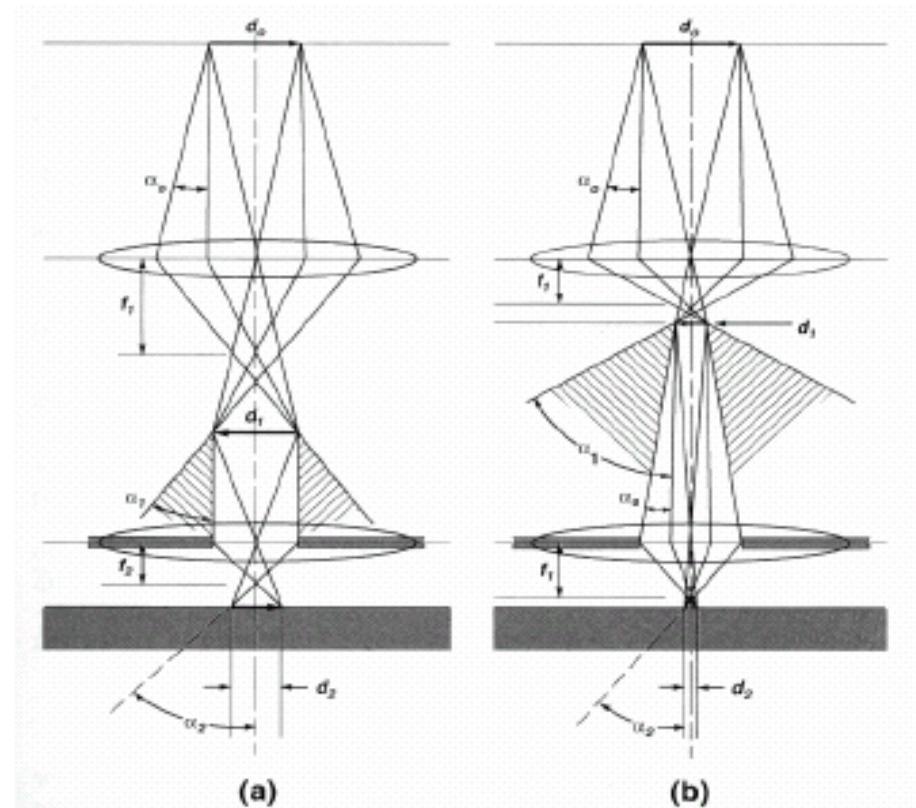
- Effects of objective lens apertures
 - Optimizes convergence angle
 - Controls depth of focus
 - Controls probe current



Larger aperture means in the case of SEM worse resolution (larger probe) but higher current

Strength of Condenser Lens

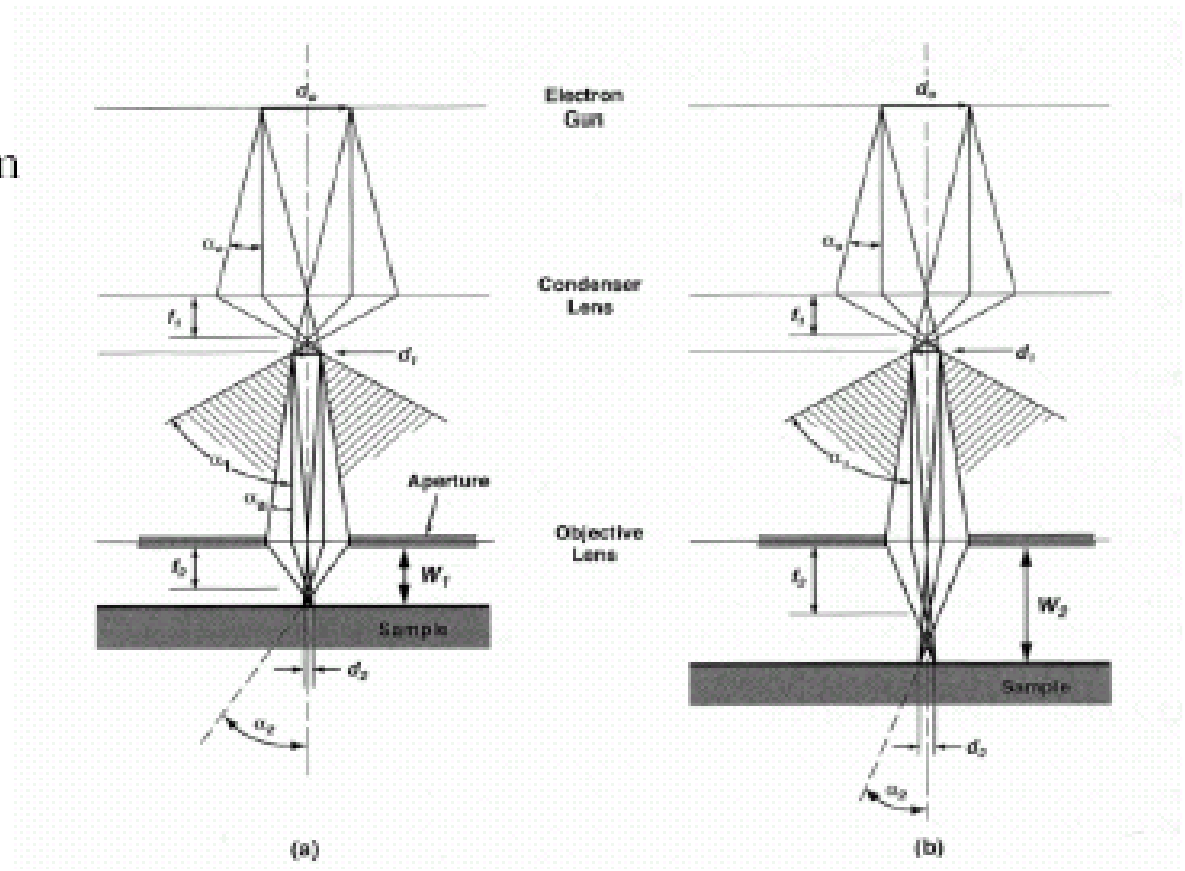
- Effects of Condenser lens strength
 - Stronger CL, smaller spot size



The effect is similar to that of changing the aperture

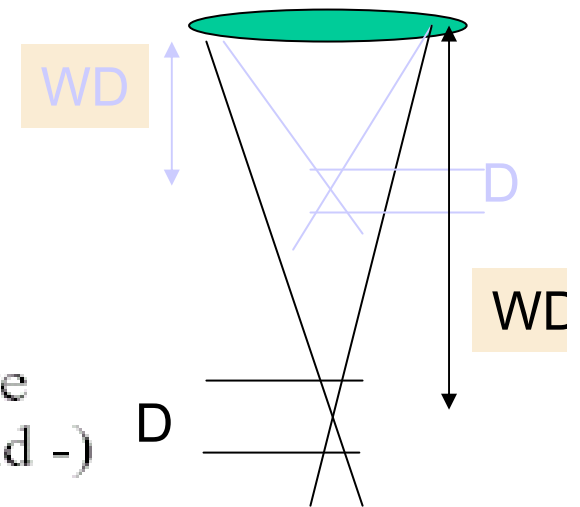
Effect of the working distance

- Effects of working distance (WD)
 - Longer WD, larger beam diameter



Depth of field

- Depth of Field - biggest advantage of SEM
 - Defined as the distance (D) between where the crossover occurs and the beam broadening is large enough that the broadening (r) is noticeable (+ and -)



$$\tan \alpha = \frac{r}{D/2}$$

$$D \approx \frac{2r}{\alpha}$$

- For CRTs, $r = 1 \text{ pixel} \sim 0.1 \text{ mm}$
- $r = 0.1 \text{ mm} / \text{Mag}$
- $D = 0.2 \text{ mm} / (\alpha * \text{Mag})$
- $\alpha = \text{Raperture} / \text{WD}$

Table 4.3. Depth of Field

Magnification	Image width (μm) ^a	Depth of Field (μm) ^b			
		$\alpha = 2 \text{ mrad}$	$\alpha = 5 \text{ mrad}$	$\alpha = 10 \text{ mrad}$	$\alpha = 30 \text{ mrad}$
10x	10,000	10,000	4000	2000	667
50x	2,000	2,000	800	400	133
100x	1,000	1,000	400	200	67
500x	200	200	80	40	13
1,000x	100	100	40	20	6.7
10,000x	10	10	4	2	0.67
100,000x	1	1	0.4	0.2	0.067

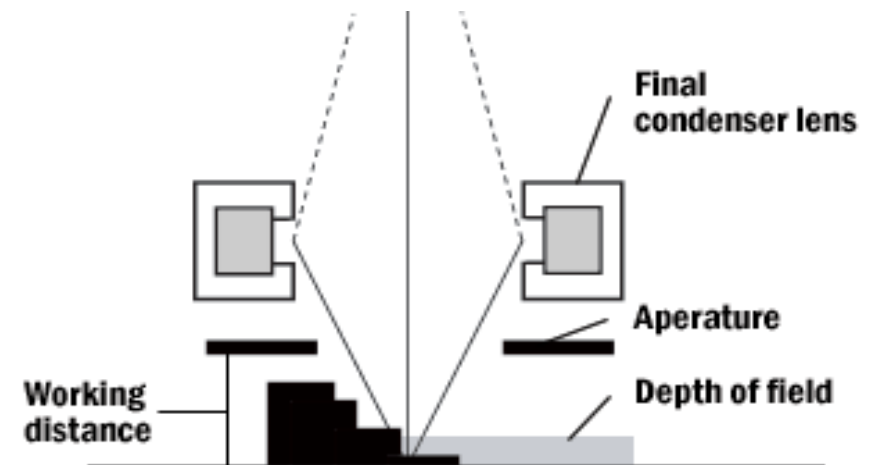
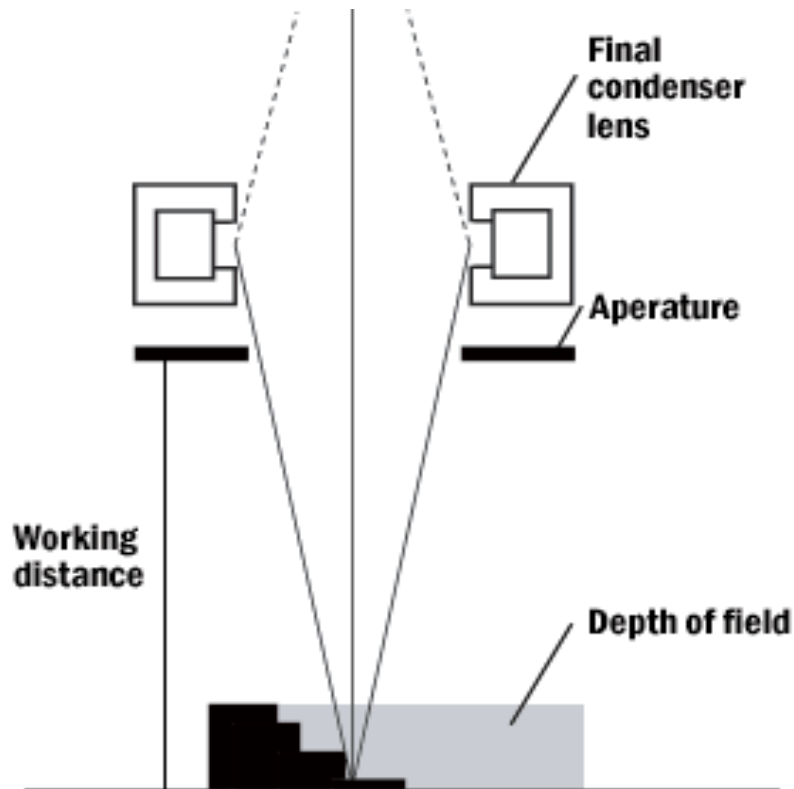
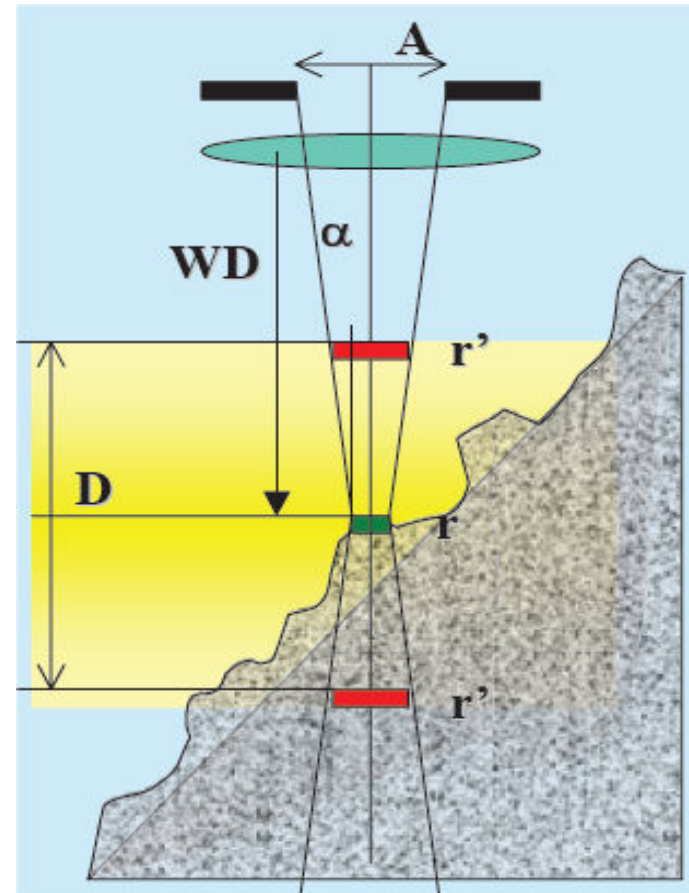
^a For a 10-cm CRT display

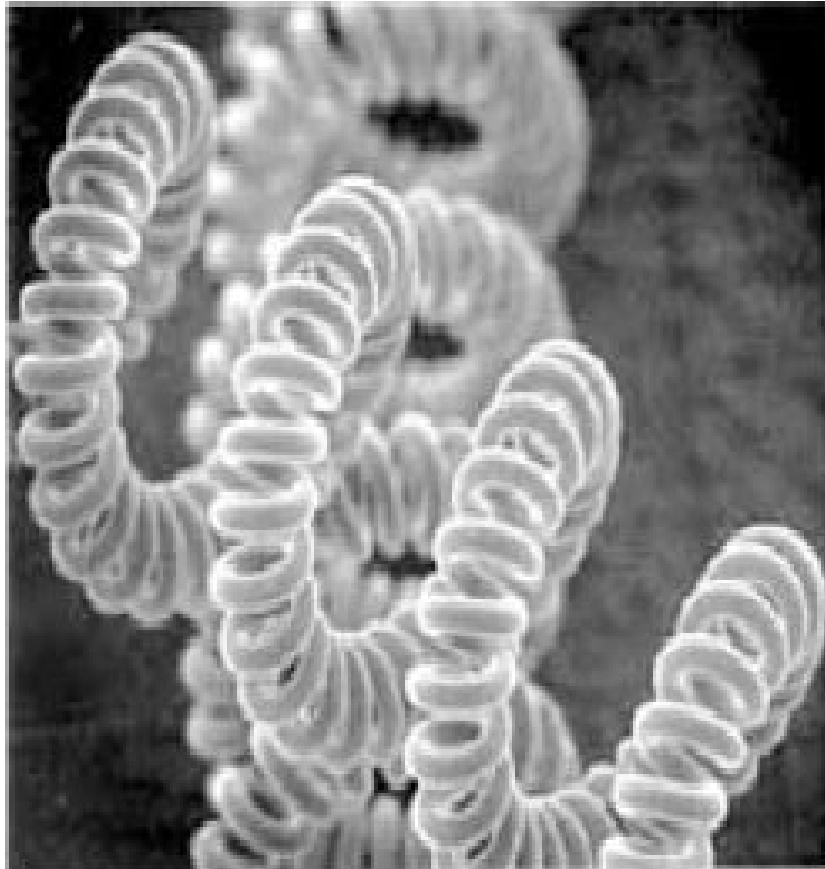
^b $\alpha = 2 \text{ mrad}$: $R_{AP} = 100 \mu\text{m}$, $D_0 = 25 \text{ mm}$; $\alpha = 5 \text{ mrad}$: $R_{AP} = 100 \mu\text{m}$, $D_0 = 10 \text{ mm}$, $d = 10 \text{ mm}$;

$R_{AP} = 200 \mu\text{m}$, $D_0 = 10 \text{ mm}$; $\alpha = 30 \text{ mrad}$: $R_{AP} = 600 \mu\text{m}$, $D_0 = 10 \text{ mm}$.

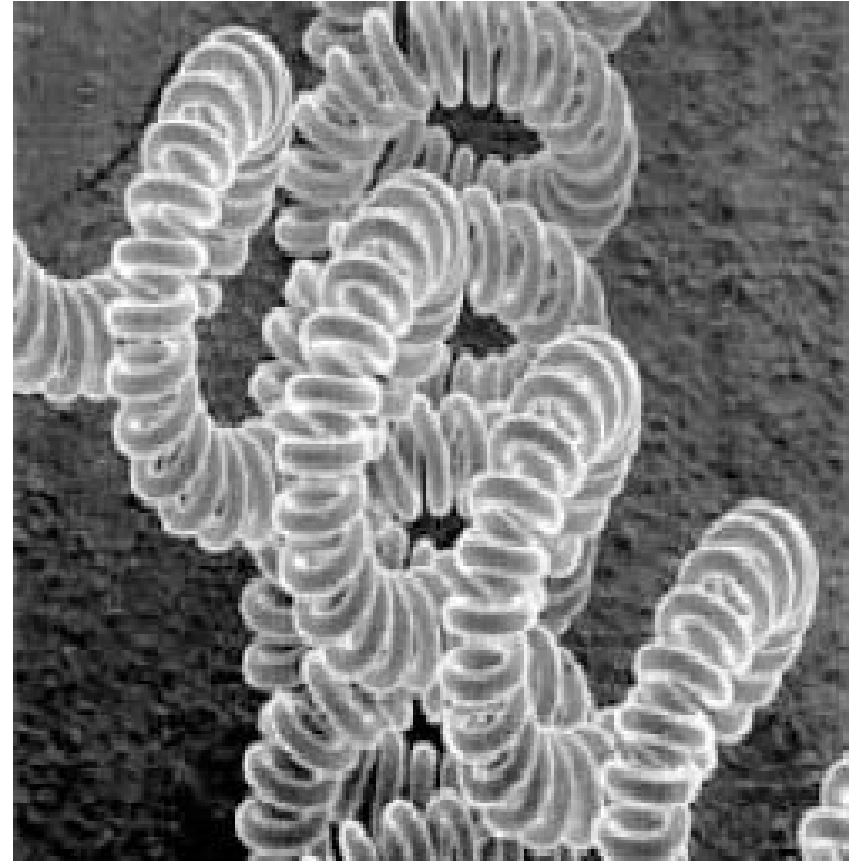
La divergenza del fascio provoca un allargamento del suo diametro sopra e sotto il punto di fuoco ottimale. In prima approssimazione, a una distanza $D/2$ dal punto di fuoco il diametro del fascio aumenta di $\Delta r \approx \alpha D/2$.

E' possibile intervenire sulla profondità di campo aumentando la distanza di lavoro e diminuendo il diametro dell'apertura finale





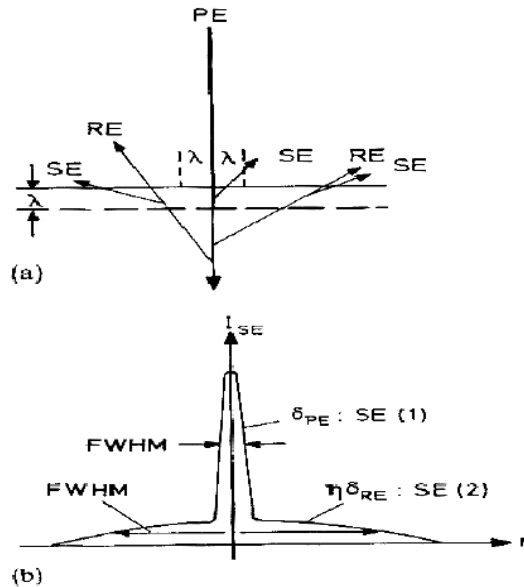
(a) OL aperture diameter: 600µm WD: 10mm



(e) OL aperture diameter: 100µm WD: 38mm

Minore e' l'apertura della lente obiettivo e maggiore e' la distanza di lavoro WD, maggiore e' la profondità di fuoco.

SECONDARY electrons



A large number of electrons of low energy $<30-50\text{eV}$ produced by the passage of the primary beam electrons.

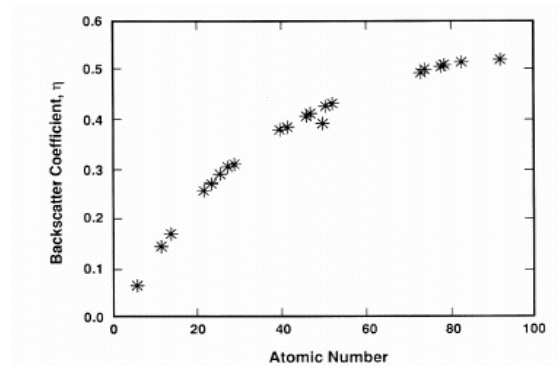
they are mainly created in a narrow area of radius λ_{SE} (few nm) = the SE creation mean free path

The **Everhart-Thornley** detectors are suited to detect these electron by means of a gate with a positive bias.

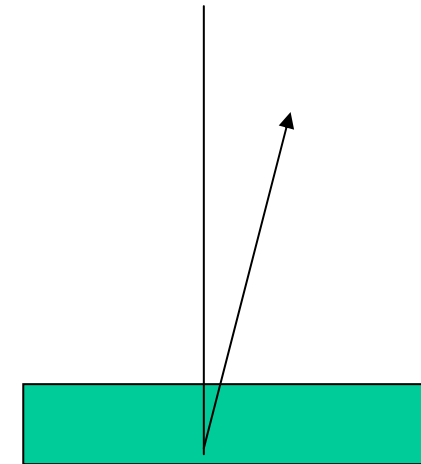
BACKSCATTERING

Backscattering coefficient=fraction of the incident beam making backscattering

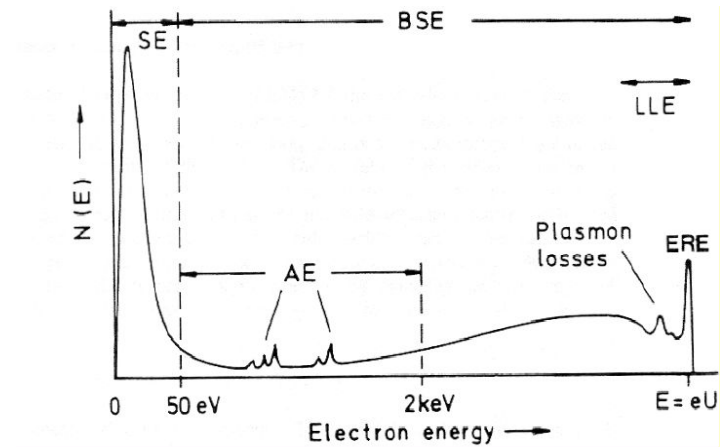
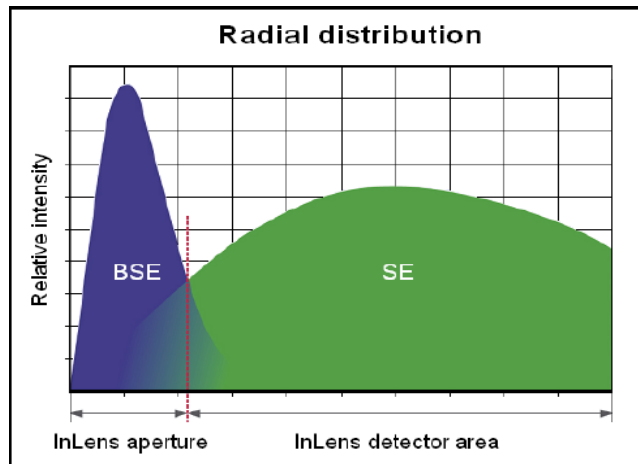
$$\eta = \frac{e^4 Z^2}{16 \pi \epsilon_0^2 E^2} \left(\frac{E + E_0}{E + 2E_0} \right)^2 Nt$$



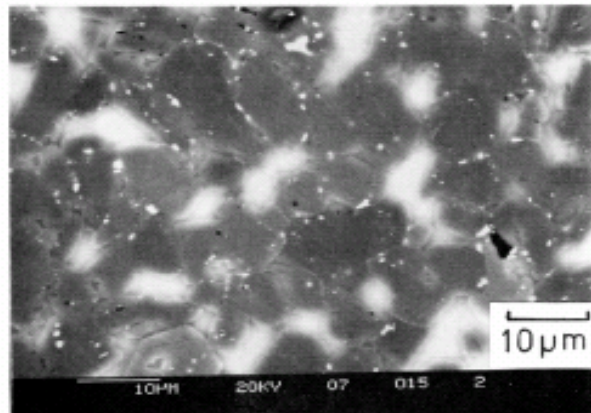
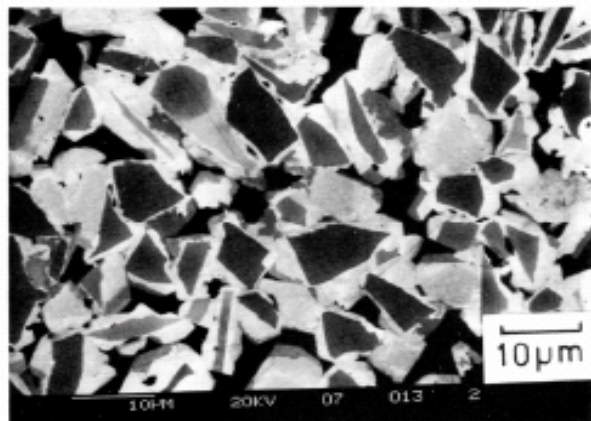
for pure compounds



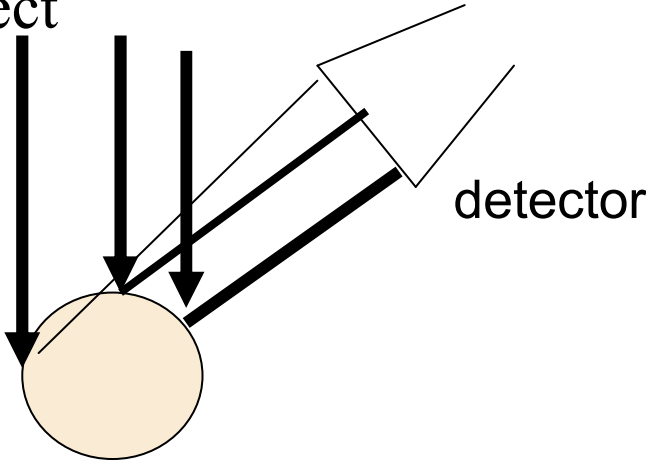
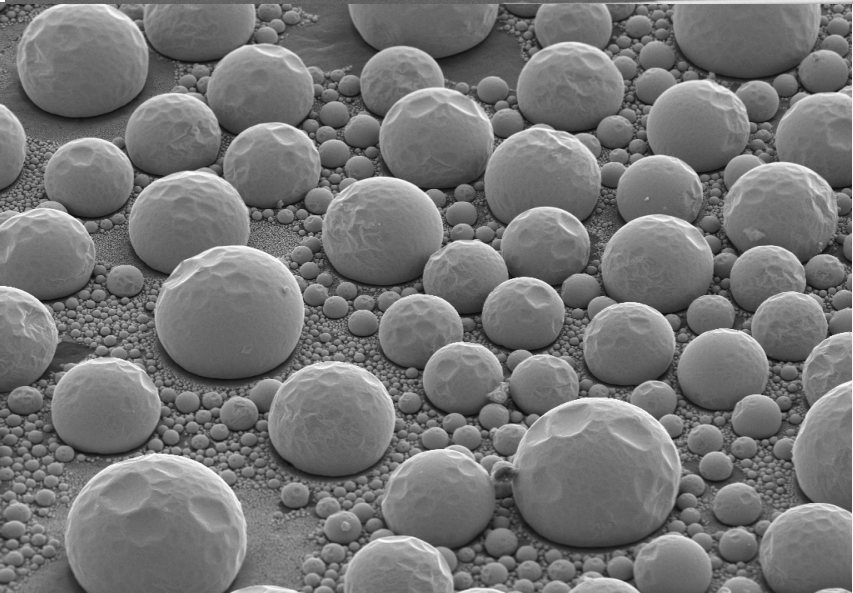
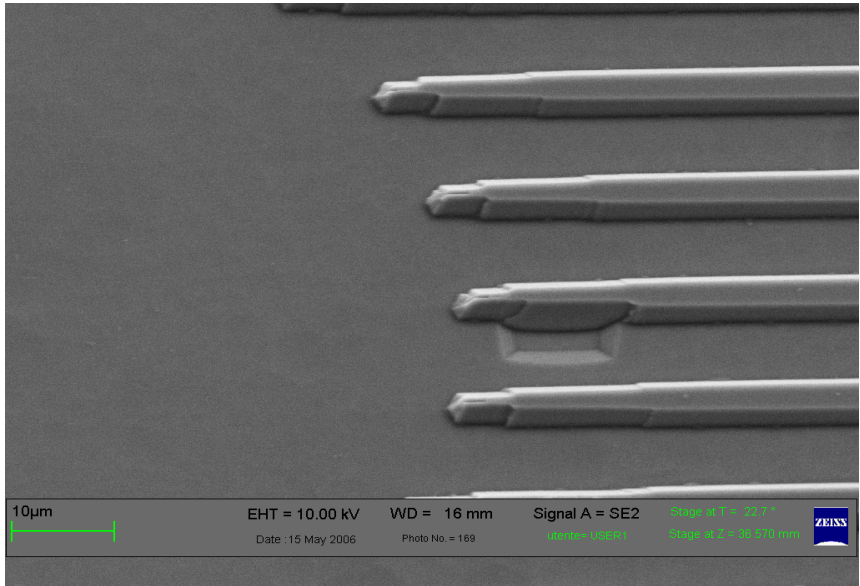
Characterised by a quite large energy



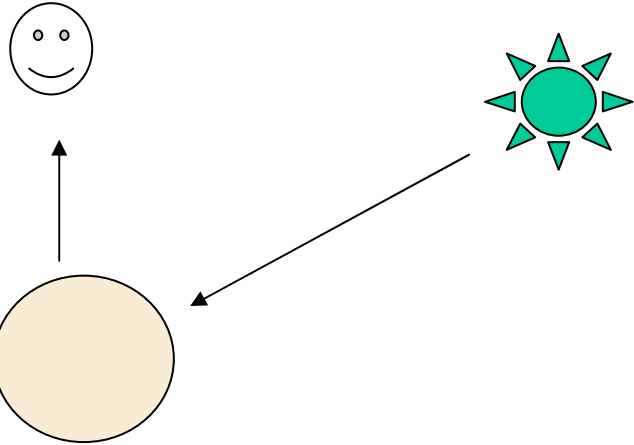
Imaging with BS and SE



Shadow effect



by reciprocity it is almost equivalent to light : most of time intuitive interpretation



channeling BSE

- e- can be Bragg diffracted by individual crystals (grains)
 - Directionality induced by diffraction gives rise to light / dark areas
 - Contrast determination? Threshold equation?
 - Best to use large solid angle BSE detector
- e- channeling can also give rise to diffraction patterns
 - Strongly affected by surface topography
 - Better to determine crystallography with EBSD

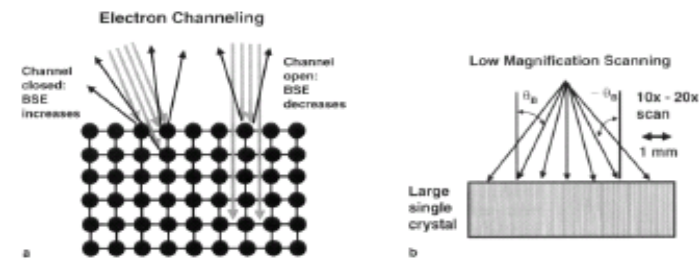


Figure 5.36. Channeling contrast. (a) Schematic diagram showing the origin of the channeling effect as penetration of the beam electrons along the crystal planes. (b) scanning at low magnification both moves the beam on the surface and changes the angle substantially across the field.

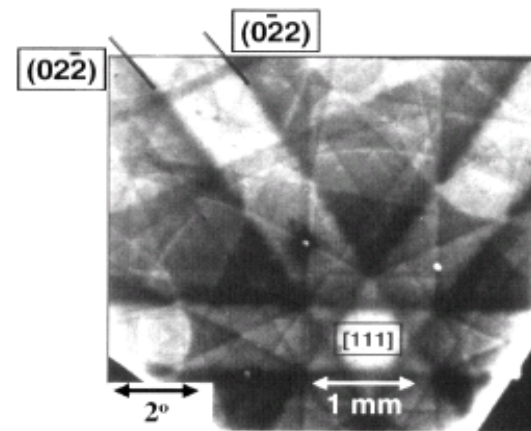
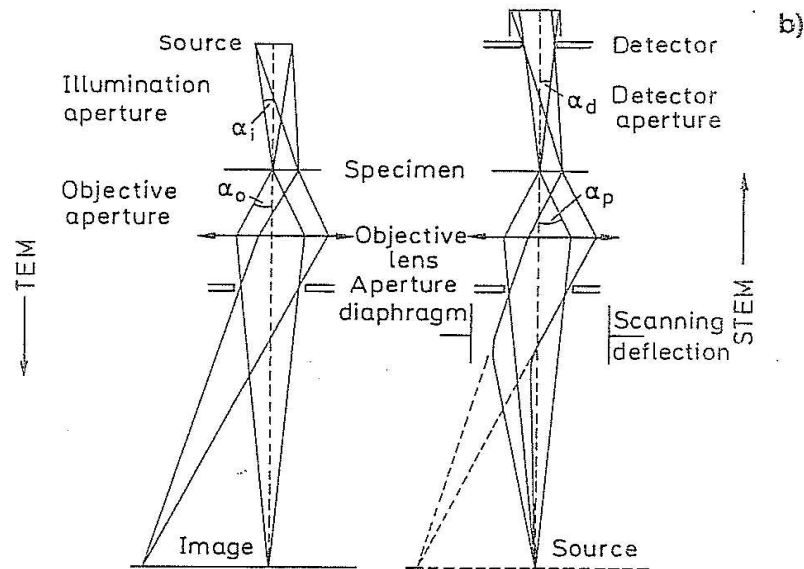


Figure 5.37. Electron channeling pattern (ECP) observed on a silicon single crystal with the [111] pole nearly parallel to the surface normal.

reciprocity principle

inverting the direction of the
electron the
image formation is equivalent



LEEM

The low energy electron microscope allows to study surfaces with 1 nm resolution. The electrons are decelerated to few tens of eV in front of the sample and reaccelerated again after being back reflected into the microscope. Contrast is achieved by selecting different diffraction channels corresponding to substrate and adsorbate or using the different reflectivity of different atomic species.